Published for SISSA by Springer

Received: *August 19, 2011*
Revised: *October 11, 2011*
Accepted: *October 11, 2011*
Published: *November 2, 2011*

Limits on scalar leptoquark interactions and consequences for GUTs

Ilja Doršner,[a] **Jure Drobnak,**[b] **Svjetlana Fajfer,**[c,b] **Jernej F. Kamenik**[b,c] **and Nejc Košnik**[d,b]

[a] *Department of Physics, University of Sarajevo, Zmaja od Bosne 33-35, 71000 Sarajevo, Bosnia and Herzegovina*
[b] *J. Stefan Institute, Jamova 39, P.O. Box 3000, 1001 Ljubljana, Slovenia*
[c] *Department of Physics, University of Ljubljana, Jadranska 19, 1000 Ljubljana, Slovenia*
[d] *Laboratoire de l'Accélérateur Linéaire, Centre d'Orsay, Université de Paris-Sud XI, B.P. 34, Bâtiment 200, 91898 Orsay cedex, France*

E-mail: ilja.dorsner@ijs.si, jure.drobnak@ijs.si, svjetlana.fajfer@ijs.si, jernej.kamenik@ijs.si, kosnik@lal.in2p3.fr

Abstract: A colored weak singlet scalar state with hypercharge 4/3 is one of the possible candidates for the explanation of the unexpectedly large forward-backward asymmetry in $t\bar{t}$ production as measured by the CDF and DØ experiments. We investigate the role of this state in a plethora of flavor changing neutral current processes and precision observables of down-quarks and charged leptons. Our analysis includes tree- and loop-level mediated observables in the K and B systems, the charged lepton sector, as well as the $Z \to b\bar{b}$ decay width. We perform a global fit of the relevant scalar couplings. This approach can explain the $(g-2)_\mu$ anomaly while tensions among the CP violating observables in the quark sector, most notably the nonstandard CP phase (and width difference) in the B_s system cannot be fully relaxed. The results are interpreted in a class of grand unified models which allow for a light colored scalar with a mass below 1 TeV. We find that the renormalizable SU(5) scenario is not compatible with our global fit, while in the SO(10) case the viability requires the presence of both the 126- and 120-dimensional representations.

Keywords: Beyond Standard Model, Rare Decays, GUT, Quark Masses and SM Parameters

ArXiv ePrint: 1107.5393

doi:10.1007/JHEP11(2011)002

JHEP11(2011)002

Contents

JHEP11(2011)002

1 Introduction

Recent CDF and DØ results on the forward-backward asymmetry (FBA) in top quark pair production have attracted a lot of attention and a number of proposals have been made in order to explain all the relevant observables (for a recent review see [1]). Among these, a colored weak singlet scalar with charge 4/3 $(\overline{\mathbf{3}}, \mathbf{1}, 4/3)$, if exchanged in the u-channel, can well accommodate most of the present measurements [2, 3] (see however also [4, 5]). Motivated by the success of this proposal [2] we have systematically investigated the role of such state in charm and top quark physics [6]. Constraints on the relevant couplings to up-type quarks come from observables related to $D^0 - \bar{D}^0$ oscillations, as well as di-jet and single top production measurements at the Tevatron and the LHC. In turn, we were able to predict the expected rates of flavor changing neutral current (FCNC) mediated top quark and charmed meson decays, generated by the presence of the new colored scalar. Due to the possibility to accommodate such states within SU(5) grand unified theories (GUTs) that contain 5- and 45-dimensional Higgs representations, we have determined the resulting textures of the up-quark mass matrix at the GUT scale. The particular SU(5) model we advocated has an appealing feature of correlating the presence of light colored scalars stemming from the 45-dimensional Higgs representation with bounds on the partial proton lifetimes. Namely, the aforementioned representation contains among other states two colored scalars—$(\overline{\mathbf{3}}, \mathbf{1}, 4/3)$ and $(\mathbf{8}, \mathbf{2}, 1/2)$—whose masses are below or of the order of 1 TeV when partial proton decay lifetimes are predicted to be at or slightly above the current experimental bounds. The most common renormalizable models based on SO(10) framework [7, 8], on the other hand, usually rely on inclusion of 120- and 126-dimensional scalar representations to generate fermion masses. As it turns out, both of these contain a colored weak singlet $(\overline{\mathbf{3}}, \mathbf{1}, 4/3)$ state that, if light, could accommodate the $t\bar{t}$ production observables [2, 9]. Our analysis of its couplings could thus help in establishing the viability of such SO(10) scenarios as we demonstrate later.

During the last decades, rare processes involving down-type quarks and charged leptons have played an important role in revealing possible signs of new physics (NP) at low energies. A prominent example is the anomalous magnetic moment of the muon, whose most precise experimental measurement [10] deviates from theoretical predictions within the SM [11] by about three standard deviations. Also most recently, the CDF and DØ experiments [12–15] have reported indications of a large CP-violating phase entering the $B_s - \bar{B}_s$ mixing amplitude, which cannot be accommodated within the standard Cabibbo-Kobayashi-Maskawa (CKM) framework.[1] Furthermore, the experimental data seem to prefer the decay widths' difference between the B_s eigenstates $\Delta\Gamma_s$ larger than predicted within the SM. Any NP addressing this discrepancy would have to contribute to the absorptive part of the mixing amplitude [20]. Finally, the recent measurements of the leptonic $B \to \tau\nu$ branching ratio induce a $2.9\,\sigma$ tension on the global fit to the CKM unitarity triangle which may be ameliorated via a small NP contribution to the B_d-$\bar{B}_d$ mixing phase [19].

[1] The recent DØ measurement of an anomalous like-sign dimuon charge asymmetry [16, 17] is consistent with the hypothesis of NP contributing only in $B_{d,s} - \bar{B}_{d,s}$ mixing [18, 19].

JHEP11(2011)002

Motivated by the interesting role the scalar $(\overline{\mathbf{3}}, \mathbf{1}, 4/3)$ state might play in down-quark and charged lepton physics, we systematically investigate its contributions to the down-quark and charged lepton physical observables. We consider observables affected already at the tree-level, as for example $K_{L,S}(B_{s,d}) \to \ell^+\ell'^-$, lepton flavor violating (LFV) tau decays and $\mu - e$ conversion in nuclei, and also loop suppressed contributions to ϵ_K, Δm_K, $B_{d,s} - \bar{B}_{d,s}$ oscillation observables, lepton anomalous magnetic moments, LFV radiative tau and muon decays, and the $Z \to b\bar{b}$ decay width. These constraints can be consistently implemented within the framework of SU(5) and SO(10) GUTs which rely on tree-level generation of charged fermion masses.

The outline of this article is as follows. In section 2 we define the leptoquark couplings of the scalar $(\bar{\mathbf{3}}, \mathbf{1}, 4/3)$ to SM fermions. In section 3 we study the effects of this state on low energy precision observables and perform a global fit of its couplings in section 4. Resulting values of couplings are then reanalyzed in section 5, where we study how they relate to the mechanism of mass generation in GUT scenarios and derive bounds on the vacuum expectation value of the 45-dimensional Higgs representation in the SU(5) case. Finally we conclude in section 6.

2 Electroweak scale framework

We consider a color triplet, weak singlet scalar with charge 4/3

$$\Delta = (\overline{\mathbf{3}}, \mathbf{1}, 4/3)\,, \tag{2.1}$$

which can couple to the right-handed fermions of the SM via the interaction Lagrangian

$$\mathcal{L}_\Delta = Y_{ij}\bar{\ell}_i P_L d^C_{ja}\Delta^{a*} + \frac{g_{ij}}{2}\epsilon_{abc}\bar{u}_{ia}P_L u^C_{jb}\Delta^c + \text{h.c.}\,, \tag{2.2}$$

where $P_{L,R} = (1 \mp \gamma_5)$ and the totally antisymmetric tensor ϵ_{abc} is defined with $\epsilon_{123} = 1$. The above interaction terms exhaust all possibilities of renormalizable couplings between SM fermions and the Δ scalar. As mentioned in section 1, the diquark couplings g_{ij} of Δ to up-quarks of different generations $u_i u_j$ can play an important role in top and charm physics. The leptoquark nature of Δ, on the other hand, is parameterized by couplings Y_{ij} to charged leptons and down-quarks, $\ell_i d_j$. If, and only if both g and Y are present, baryon (B) and lepton (L) numbers are violated while their combination $B - L$ is conserved. Proton lifetime is protected in this general case by antisymmetric color contraction between Δ and two up-quarks. It implies flavor-space antisymmetric coupling $g_{ij}(= -g_{ji})$ which prohibits the proton from decaying via dimension-6 effective operators mediated by Δ. To comply with the $t\bar{t}$ production parameters, the mass of Δ should be below 1 TeV, preferably around 400 GeV. This setup is natural in a theoretically well-motivated class of grand unified models. A realistic GUT context of (2.2) and the resulting model building constraints will be presented in section 5.

In general Y is a complex matrix acting on charged-lepton and down-quark flavor indices $\bar{\ell}_R Y (d_R)^C$. From the right-hand side of Y one may redefine the quark fields using the global B symmetry transformation, which since it is broken, has a side effect of globally

JHEP11(2011)002

rephasing diquark couplings g while leaving the mass and CKM matrices invariant. This is not a worry at this point since current experimental constraints from top quark physics and $D^0 - \bar{D}^0$ mixing observables cannot probe the overall phase of g [6]. One can redefine lepton fields in an analogous manner. However, of the two independent phases used to redefine quark and lepton fields only their sum is physical, while their difference corresponds to $B - L$, a conserved quantum number. As a result, freedom remains to choose one phase in Y. Strictly speaking, from the phenomenological point of view in section 3 where we do not consider observables sensitive to lepton mixing, we could have rephased charged lepton flavors independently. This would allow us to rephase each row of Y separately. We restrain however from using this freedom which would result in the leptonic phase convention being "gauged" according to Y instead of to the standard form of the Pontecorvo-Maki-Nakagawa-Sakata (PMNS) matrix.

3 Leptoquark probing observables

The leptoquark couplings endow the scalar Δ with a potential to cause large effects in (flavor changing) neutral current processes of down quarks and charged leptons (see [21] for a recent analysis of scalar leptoquark constraints from K and B sectors). The couplings Y_{ij} of eq. (2.2) must therefore pass constraints from plethora of precisely measured or bounded low energy observables. In this section we make predictions of the observables most sensitive to effects stemming from Δ and compare them to current experimental values. For each observable we state an effective error of the constraint, which is, as will be explained in the following, a total combined theoretical and experimental uncertainty. In order to confront this model with experimental data in a quantitative manner we wrap up the analysis with a global fit of all the 9 entries of Y in section 4.

3.1 SM theoretical inputs

Most observed flavor phenomena are well described within the SM and thus the allowed size of NP contributions crucially depends on reliable estimates of SM parameters. In the presence of NP virtual contributions to quark flavor observables the extraction of the CKM matrix becomes more involved, since some observables used in the conventional CKM fits receive contributions from both the SM and NP amplitudes. As we want to treat the SM contributions as a theoretical background, it is imperative to calibrate the CKM matrix exclusively on SM tree-level observables, which are largely insensitive to virtual Δ contributions.

Thus we employ the results of a simple CKM fit to tree-level observables.[2] These are the measurements of the first and the second row CKM element moduli from super-allowed β decays, leptonic and semileptonic meson decays, as well as the extraction of the CP phase

[2]We do not use available results in the literature since they do not provide correlations among the parameters (e.g. UTFit tree-level fit [22]).

JHEP11(2011)002

angle γ from tree-dominated B decays [23]

$$|V_{\rm CKM}| = \begin{pmatrix} 0.97425(22) & 0.2252(9) & 3.89(44)\times 10^{-3} \\ 0.23(11) & 1.023(36) & 4.06(13)\times 10^{-2} \\ & & \end{pmatrix}, \qquad \gamma = 73(^{+22}_{-25})^\circ . \tag{3.1}$$

In particular, the value of $|V_{ub}|$ is an average of exclusive and inclusive semileptonic B decay analyses. We explore the impact of the branching ratio of $B \to \tau\nu$ on the CKM fit in section 4.2. Note that we cannot use direct $|V_{tb}|$ determination from single top production measurements, since these may be affected by Δ contributions [6]. By fitting constraints (3.1) to the Wolfenstein expanded CKM matrix up to order λ^4, we find values in agreement with [22]

$$\begin{aligned} \lambda &= 0.22538(65)\,, \\ A &= 0.799(26)\,, \\ \rho &= 0.124(70)\,, \\ \eta &= 0.407(52)\,, \end{aligned} \tag{3.2}$$

while we also extract the correlation matrix between the fit parameters

$$\begin{pmatrix} 1 & & & \\ -0.178 & 1 & & \\ -0.00517 & -0.0553 & 1 & \\ -0.0226 & -0.242 & -0.198 & 1 \end{pmatrix}. \tag{3.3}$$

In addition, we use the top quark pole mass of $m_t = 173.3\,\text{GeV}$ [24], and the $\overline{\rm MS}$ bottom and charm quark masses $m_b(m_b) = 4.2\,\text{GeV}$, and $m_c(m_c) = 1.29\,\text{GeV}$ [23]. Observable-specific numerical inputs will be stated where needed.

3.2 Tree-level constraints

We first focus our attention on observables which receive possible Δ contributions already at the tree-level and thus represent potentially most severe constraints on the Y matrix. The relevant effective Lagrangian for processes involving charged lepton and down-quark pairs results from integrating out the Δ at tree level. After applying Fierz identities we recover the LFV and quark FCNC interaction terms among the right-handed leptons and quarks

$$\mathcal{L}^{\Delta}_{d_i\bar{d}_j\to\ell_a^-\ell_b^+} = -\frac{Y_{aj}Y^*_{bi}}{2m^2_\Delta}(\bar{\ell}_a\gamma^\mu P_R\ell_b)(\bar{d}_j\gamma_\mu P_R d_i)\,. \tag{3.4}$$

The corresponding leptonic (LFV) decay width of a neutral pseudoscalar meson $P(d_i\bar{d}_j) \to \ell_a^-\ell_b^+$ is given by

$$\Gamma_{P(d_i\bar{d}_j)\to\ell_a^-\ell_b^+} = \frac{|Y_{aj}Y^*_{bi}|^2}{512\pi}\frac{m_P^3 f_P^2}{m^4_\Delta}\left[\hat{m}_a^2+\hat{m}_b^2-(\hat{m}_a^2-\hat{m}_b^2)^2\right]\left[(1-(\hat{m}_a+\hat{m}_b)^2)(1-(\hat{m}_a-\hat{m}_b)^2)\right]^{1/2}, \tag{3.5}$$

where m_P is the decaying meson mass, its decay constant is defined as customary for light neutral mesons (π^0, K^0), $\langle 0 \,|\, \bar{d}_j\gamma^\mu\gamma_5 d_i \,|\, P(p)\rangle = ip^\mu f_P/\sqrt{2}$, while the hatted masses of leptons are $\hat{m}_{a,b} = m_{a,b}/m_P$. We study the particularly interesting decay modes below.

JHEP11(2011)002

3.2.1 $K_L \to \mu^-\mu^+,\ e^+e^-,\ \mu^\pm e^\mp$

While the decay $K_L \to \mu^-\mu^+$ has been measured with great precision ($\mathcal{B} = (6.84 \pm 0.11) \times 10^{-9}$ [23]), the presence of long-distance intermediate states $K_L \to \gamma^*\gamma^* \to \mu^+\mu^-$ precludes similarly reliable SM predictions for this observable. We use a conservative estimate for the pure short distance branching fraction $\mathcal{B}_{\rm SD}^{\rm exp} < 2.5 \times 10^{-9}$, obtained using dispersive techniques [25, 26], as a $1\,\sigma$ upper bound. Since the SM short distance contribution $\mathcal{B}_{\rm SM(SD)} \approx 0.9 \times 10^{-9}$ is much smaller, we can neglect it and keep only the Δ-mediated amplitude. For the decay width $K_L \to \mu^+\mu^-$, CP violation in $K - \bar{K}$ mixing is irrelevant and we treat K_L as a pure CP-odd state. Contributions of both K^0 and $\bar{K}^0$ amplitudes are to be taken into account using eq. (3.5) by replacing $Y_{aj}Y_{bi}{}^* \to \sqrt{2}\mathrm{Re}(Y_{\mu s}Y_{\mu d}{}^*)$. The decay width, mediated by CP conserving combination of couplings Y, is then

$$\Gamma_{K_L\to\mu^-\mu^+} = \frac{\left[\mathrm{Re}\left(Y_{\mu s}Y_{\mu d}^*\right)\right]^2}{128\pi}\frac{m_K^3 f_K^2}{m_\Delta^4}\hat{m}_\mu^2\sqrt{1-4\hat{m}_\mu^2}\,. \tag{3.6}$$

Using the lattice value of the kaon decay constant $f_K = 156.0\,\mathrm{MeV}$ [27], the numerical result for the $1\,\sigma$ upper bound is

$$\left[\mathrm{Re}\left(Y_{\mu s}Y_{\mu d}^*\right)\right]^2 < 2.7 \times 10^{-9}\left(\frac{m_\Delta}{400\ \mathrm{GeV}}\right)^4. \tag{3.7}$$

In the di-electron mode $K_L \to e^+e^-$ the experimental measurement of $\mathcal{B} = (9^{+6}_{-4}) \times 10^{-12}$ [23] agrees well with the long-distance dominated SM estimate of $\mathcal{B}_{\rm LD}^{\rm SM} = (9 \pm 0.5) \times 10^{-12}$ [28]. The Δ contribution to this decay mode can be obtained from (3.6) by replacing μ with e everywhere. Saturating the experimental uncertainty leads to the following $1\,\sigma$ constraint

$$\left[\mathrm{Re}\left(Y_{es}Y_{ed}^*\right)\right]^2 < 2.5 \times 10^{-7}\left(\frac{m_\Delta}{400\ \mathrm{GeV}}\right)^4. \tag{3.8}$$

A much stronger upper bound of the LFV decays $\mathcal{B}(K_L \to \mu^\pm e^\mp) < 4.7 \times 10^{-12}$ at 90% confidence level (C.L.) has been set in [23]. The corresponding form of eq. (3.5) is obtained by adding first coherently the flavor components of K_L and then summing over the widths of the two oppositely-charged final states. The result, with m_e set to zero, is

$$\Gamma_{K_L\to\mu^\pm e^\mp} = \frac{|Y_{\mu s}Y_{ed}^* + Y_{\mu d}Y_{es}^*|^2}{512\pi}\frac{m_K^3 f_K^2}{m_\Delta^4}\hat{m}_\mu^2\left[1-\hat{m}_\mu^2\right]^2, \tag{3.9}$$

and implies a $1\,\sigma$ bound

$$|Y_{\mu s}Y_{ed}^* + Y_{\mu d}Y_{es}^*|^2 < 1.2 \times 10^{-11}\left(\frac{m_\Delta}{400\ \mathrm{GeV}}\right)^4. \tag{3.10}$$

3.2.2 $K_S \to e^-e^+, \mu^+\mu^-$

Since K_S is approximately CP-even and is decaying to a CP-odd final state this decay mode is sensitive to the imaginary parts of Y. In the muonic channel, the best limit still comes from the early seventies with $\mathcal{B}(K_S \to \mu^+\mu^-) < 3.2 \times 10^{-7}$ at 90 % C.L. [23], while the best upper bound on the branching fraction $\mathcal{B}(K_S \to e^+e^-) < 9 \times 10^{-9}$ at 90 % C.L. was more

JHEP11(2011)002

recently set by the KLOE experiment [29]. Both are still far above the SM expectations, whose long distance effects through $K_S \to \gamma^*\gamma^* \to e^-e^+(\mu^+\mu^-)$ reach $8\times10^{-9}(2\times10^{-6})\times \mathcal{B}(K_S \to \gamma\gamma) \sim 10^{-14}(10^{-11})$ [23, 30]. These observables thus present clean probes of CP violating effects in the effective Lagrangian (3.4), through the decay widths

$$\Gamma_{K_S\to e^-e^+} = \frac{\left[\mathrm{Im}\left(Y_{es}Y^*_{ed}\right)\right]^2}{128\pi}\frac{m_K^3 f_K^2}{m_\Delta^4}\hat{m}_e^2\,, \tag{3.11}$$

$$\Gamma_{K_S\to \mu^-\mu^+} = \frac{\left[\mathrm{Im}\left(Y_{\mu s}Y^*_{\mu d}\right)\right]^2}{128\pi}\frac{m_K^3 f_K^2}{m_\Delta^4}\hat{m}_\mu^2\sqrt{1-4\hat{m}_\mu^2}\,. \tag{3.12}$$

The resulting bounds, although diluted by helicity suppression in the electron mode and the short lifetime of K_S, are important constraints to be fulfilled by the following combinations of couplings at $1\,\sigma$ C.L.

$$\left[\mathrm{Im}\left(Y_{es}Y^*_{ed}\right)\right]^2 < 0.13\left(\frac{m_\Delta}{400\ \mathrm{GeV}}\right)^4, \tag{3.13}$$

$$\left[\mathrm{Im}\left(Y_{\mu s}Y^*_{\mu d}\right)\right]^2 < 1.1\times10^{-4}\left(\frac{m_\Delta}{400\ \mathrm{GeV}}\right)^4. \tag{3.14}$$

3.2.3 $B_{d(s)} \to \ell^-\ell^+$

In the SM these FCNC processes suffer additional helicity-suppression (m_ℓ^2/m_B^2) leading to branching fractions of the modes with electrons, which are negligibly small compared to the current sensitivities of experiments, as given by the 90 % C.L. upper bounds on $\mathcal{B}(B_d \to e^-e^+) < 8.3\times10^{-8}$ and $\mathcal{B}(B_s \to e^-e^+) < 2.8\times10^{-7}$ [23]. In the dimuon channel the SM predictions for the branching fractions — of order $\sim 10^{-10}$ (10^{-9}) for B_d (B_s) decays — are closer to but still an order of magnitude below current experimental 90 % C.L. upper bounds 4.2×10^{-9} (1.2×10^{-8}) [31]. Even in the case of $B_d \to \tau^-\tau^+$ where the helicity suppression is the least severe, the SM prediction of $\mathcal{B} \sim 10^{-7}$ [32] is far below the current experimental reach of 4.1×10^{-3} at 90 % C.L. [33]. Consequently we do not need to consider pure SM or interference terms between SM and Δ-mediated amplitudes and focus our attention only to the pure Δ contributions.

In eq. (3.5) we substitute $f_P \to \sqrt{2}f_{B_{d(s)}}$ in order to conform with the standard normalization of heavy pseudoscalar decay constants. The lepton flavor conserving decay widths then read

$$\Gamma_{B_{d(s)}\to\ell^-\ell^+} = \frac{\left|Y_{\ell b}Y^*_{\ell d(s)}\right|^2}{128\pi}\frac{m^3_{B_{d(s)}} f^2_{B_{d(s)}}}{m_\Delta^4}\hat{m}_\ell^2\sqrt{1-4\hat{m}_\ell^2}\,, \tag{3.15}$$

while the rates of LFV decays are, e.g., for the $\mu\tau$ final state

$$\Gamma_{B_d\to\tau^-\mu^+} = \frac{\left|Y_{\tau b}Y^*_{\mu d}\right|^2}{256\pi}\frac{m^3_{B_d} f^2_{B_d}}{m_\Delta^4}\hat{m}_\tau^2(1-\hat{m}_\tau^2)\,. \tag{3.16}$$

For the other dilepton LFV decays one should adapt the lepton indices of Y and replace $\hat{m}_\tau$ with the mass of the heaviest lepton in the final state. For the decay constants we use the central values of recent lattice QCD averages [27]: $f_{B_d} = 193\,\mathrm{MeV}$, $f_{B_s} = 239\,\mathrm{MeV}$. The compilation of experimental upper bounds and their resulting interpretation as constraints on Y are given in table 1.

JHEP11(2011)002

decay mode	90 % C.L. exp. bound on $\mathcal{B}$	$1\,\sigma$ upper bound in units $(m_\Delta/400\ \text{GeV})^4$
$B_d \to e^- e^+$	8.3×10^{-8}	$\lvert Y_{eb} Y^*_{ed}\rvert^2 < 4.4$
$B_d \to \mu^- \mu^+$	4.2×10^{-9}	$\left\lvert Y_{\mu b} Y^*_{\mu d}\right\rvert^2 < 5.0 \times 10^{-6}$
$B_d \to \tau^- \tau^+$	4.1×10^{-3}	$\lvert Y_{\tau b} Y^*_{\tau d}\rvert^2 < 1.3 \times 10^{-2}$
$B_s \to e^- e^+$	2.8×10^{-7}	$\lvert Y_{eb} Y^*_{es}\rvert^2 < 10.1$
$B_s \to \mu^- \mu^+$	1.2×10^{-8}	$\left\lvert Y_{\mu b} Y^*_{\mu s}\right\rvert^2 < 1.1 \times 10^{-5}$
$B_d \to e^\mp \mu^\pm$	6.4×10^{-8}	$\left\lvert Y_{eb} Y^*_{\mu d}\right\rvert^2 + \lvert Y_{\mu b} Y^*_{ed}\rvert^2 < 1.6 \times 10^{-4}$
$B_d \to \mu^\mp \tau^\pm$	2.2×10^{-5}	$\lvert Y_{\mu b} Y^*_{\tau d}\rvert^2 + \left\lvert Y_{\tau b} Y^*_{\mu d}\right\rvert^2 < 2.2 \times 10^{-4}$
$B_d \to \tau^\mp e^\pm$	2.8×10^{-5}	$\lvert Y_{\tau b} Y^*_{ed}\rvert^2 + \lvert Y_{eb} Y^*_{\tau d}\rvert^2 < 2.7 \times 10^{-4}$
$B_s \to e^\mp \mu^\pm$	2.0×10^{-7}	$\left\lvert Y_{eb} Y^*_{\mu s}\right\rvert^2 + \lvert Y_{\mu b} Y^*_{es}\rvert^2 < 3.4 \times 10^{-4}$

Table 1. Limits on Y couplings coming from upper bounds of lepton flavor conserving and violating $B_{d(s)} \to \ell^- \ell^+$ decays [23, 31].

3.2.4 $B \to X_s \ell^+ \ell^-$

Effective Lagrangian (3.4) also contributes to the non-helicity suppressed $b \to s\ell^+\ell^-$ transitions. In particular it contributes to the $C_{9'}$ and $C_{10'}$ Wilson coefficients of the effective weak Hamiltonian as defined in [34]. Following this reference, we write

$$\mathcal{H}_{\text{eff}}^{(bs)} = -\frac{4G_F}{\sqrt{2}} \lambda_t^{(s)} \sum_i C_i^\ell \mathcal{O}_i^\ell \,, \tag{3.17}$$

where $\lambda_t^{(s)} = V_{tb} V_{ts}^*$, and Δ only contributes to

$$\mathcal{O}_{9'}^\ell = \frac{e^2}{16\pi^2} (\bar{s}\gamma_\mu P_R b)(\bar{\ell}\gamma^\mu \ell) \,, \qquad \mathcal{O}_{10'}^\ell = \frac{e^2}{16\pi^2} (\bar{s}\gamma_\mu P_R b)(\bar{\ell}\gamma^\mu \gamma_5 \ell) \,, \tag{3.18}$$

at the tree-level with the weak-scale Wilson coefficients

$$C_{9'}^\ell = C_{10'}^\ell = -\frac{\sqrt{2}\pi Y_{\ell b} Y_{\ell s}^*}{4G_F \lambda_t^{(s)} \alpha\, m_\Delta^2} \,. \tag{3.19}$$

The running of the $O_{9',10'}^\ell$ operators from the weak matching scale to the b-quark mass scale is dominated by electroweak effects [35] and can be safely neglected for our purpose. At present the most sensitive observable is the inclusive decay width of $B \to X_s \ell^+ \ell^-$, where $\ell = e, \mu$, integrated in the dilepton invariant mass range of $m_{\ell^+\ell^-} \equiv \sqrt{(p_{\ell^+} + p_{\ell^-})^2} \in [1, 6]\,\text{GeV}$. The corresponding branching fraction ($\mathcal{B}_{(1-6)\text{GeV}}$) is known in the SM to 10% accuracy and can be written in presence of $C_{9',10'}$ contributions as [34]

$$\mathcal{B}^{\text{th}}_{(1-6)\text{GeV}} = \left| \frac{\lambda_t^{(s)}/V_{cb}}{0.981} \right|^2 [(15.86 \pm 1.51) - 0.049\,\text{Re}(C_{9'}^\ell) + 0.061\,\text{Re}(C_{10'}^\ell) + 0.534 |C_{9'}^\ell|^2 + 0.543 |C_{10'}^\ell|^2] \times 10^{-7} \,. \tag{3.20}$$

The experimental measurements of this quantity by the BaBar [36] and Belle [37] experiments, averaged over the muon and electron flavors, yield $\mathcal{B}^{\text{exp}}_{(1-6)\text{GeV}} = (1.60 \pm 0.5) \times 10^{-6}$ [38].

JHEP11(2011)002

decay mode	90 % C.L. exp. bound on $\mathcal{B}$	$1\,\sigma$ upper bound in units $(m_\Delta/400\ \text{GeV})^4$
$B^+ \to \pi^+\ell^-\ell^+$	4.9×10^{-8}	$\lvert Y_{eb}Y^*_{ed}\rvert^2 + \left\lvert Y_{\mu b}Y^*_{\mu d}\right\rvert^2 < 3.0 \times 10^{-7}$
$B^+ \to \pi^+ e^\pm\mu^\mp$	1.7×10^{-7}	$\left\lvert Y_{eb}Y^*_{\mu d}\right\rvert^2 + \lvert Y_{\mu b}Y^*_{ed}\rvert^2 < 1.1 \times 10^{-6}$
$B^+ \to K^+ e^\pm\mu^\mp$	9.1×10^{-8}	$\left\lvert Y_{eb}Y^*_{\mu s}\right\rvert^2 + \lvert Y_{\mu b}Y^*_{es}\rvert^2 < 4.3 \times 10^{-7}$
$B^+ \to K^+\tau^\pm\mu^\mp$	7.7×10^{-5}	$\left\lvert Y_{\tau b}Y^*_{\mu s}\right\rvert^2 + \lvert Y_{\mu b}Y^*_{\tau s}\rvert^2 < 5.7 \times 10^{-4}$

Table 2. Limits on Y couplings coming from upper bounds on $B^+ \to \pi(K)\ell^-\ell'^+$ branching fractions, compiled by [23].

3.2.5 $B \to \pi\ell^+\ell'^-$ and $B \to K\ell^+\ell'^-$

The exclusive $B \to \pi\ell^+\ell^-$ mode, where $\ell = \mu, e$, is severely CKM suppressed in the SM leading to branching ratio predictions which are well below the present experimental bound $\mathcal{B}(B^+ \to \pi^+\ell^-\ell^+) < 4.9 \times 10^{-8}$ @ 90% C.L. [23]. In addition, several LFV $B^+ \to \pi^+(K^+)\ell^+\ell'^-$ modes have also been searched for at the B-factories and we compile the present bounds in table 2.

The computation of the Δ contributions to these exclusive rare semileptonic B decays requires the knowledge of the relevant hadronic $\langle\pi|\mathcal{J}^\mu_d|B\rangle$ and $\langle K|\mathcal{J}^\mu_s|B\rangle$ matrix elements, where $\mathcal{J}^\mu_q = \bar{b}\gamma_\mu P_R q$ is the relevant quark current operator. We employ the form factor parametrization

$$\langle P_q(p')|\,\bar{b}\gamma^\mu q\,|B(p)\rangle = f_+^{P_q}(s)\left[(p+p')^\mu - \frac{m_B^2 - m_{P_q}^2}{s}(p-p')^\mu\right] + f_0^{P_q}(s)\frac{m_B^2 - m_{P_q}^2}{s}(p-p')^\mu\,, \tag{3.21}$$

for $P_d \equiv \pi$ and $P_s \equiv K$, where $s = (p-p')^2$. The $f^K_{+,0}$ form factors have been computed using QCD sum rules techniques and we employ the results of [39]. For the $f^\pi_{+,0}$ form factors we use a more recent calculation [40]. The $B \to K\tau^\pm\mu^\mp$ differential decay rate can be written in a compact form by neglecting the small muon mass

$$\begin{aligned}\frac{d\Gamma}{ds}(B \to K\tau^\pm\mu^\mp) = &\frac{|Y_{\mu s}Y^*_{\tau b}|^2 + |Y_{\mu b}Y^*_{\tau s}|^2}{(16\pi)^3 m_\Delta^4} m_B^3 \lambda^{1/2} \\ &\times \left(1 - \frac{m_\tau^2}{s}\right)^2 \left[\frac{\lambda}{3} f_+^K(s)^2\left(2 + \frac{m_\tau^2}{s}\right) + \frac{m_\tau^2}{s} f_0^K(s)^2\left(1 - \frac{m_K^2}{m_B^2}\right)^2\right],\end{aligned} \tag{3.22}$$

where $\lambda \equiv \lambda(1, m_K^2/m_B^2, s/m_B^2)$ and $\lambda(a,b,c) = a^2 + b^2 + c^2 - 2(ab + bc + ca)$. For the modes without tau leptons in the final state one can neglect lepton masses completely, i.e.

$$\frac{d\Gamma}{ds}(B \to Ke^\pm\mu^\mp) = \frac{|Y_{\mu s}Y^*_{eb}|^2 + |Y_{\mu b}Y^*_{es}|^2}{(16\pi)^3 m_\Delta^4} m_B^3 \lambda^{3/2} \frac{2}{3} f_+^K(s)^2\,. \tag{3.23}$$

The modes with a pion in the final state can then be simply obtained from the above formula by replacing s with d and K with π. Integrating over the available phase space and comparing to the experimental upper bounds on $B^+ \to \pi(K)\ell^-\ell'^+$ decays [23], we obtain the constraints listed in table 2. Finally we note that the corresponding rare $K \to \pi\ell^+\ell'^-$

JHEP11(2011)002

decay mode	90 % C.L. exp. bound on $\mathcal{B}$	$1\,\sigma$ upper bound in units $(m_\Delta/400\text{ GeV})^4$
$\tau \to e\pi^0$	8.0×10^{-8}	$\lvert Y_{ed}Y^*_{\tau d}\rvert^2 < 1.9 \times 10^{-4}$
$\tau \to \mu\pi^0$	1.1×10^{-7}	$\lvert Y_{\mu d}Y^*_{\tau d}\rvert^2 < 2.7 \times 10^{-4}$
$\tau \to eK_S$	3.3×10^{-8}	$\lvert Y_{ed}Y^*_{\tau s} - Y_{es}Y^*_{\tau d}\rvert^2 < 3.2 \times 10^{-5}$
$\tau \to \mu K_S$	4.0×10^{-8}	$\lvert Y_{\mu d}Y^*_{\tau s} - Y_{\mu s}Y^*_{\tau d}\rvert^2 < 4.0 \times 10^{-5}$
$\tau \to \mu\eta$	6.5×10^{-8}	$\lvert 0.69\, Y_{\mu d}Y^*_{\tau d} - Y_{\mu s}Y^*_{\tau s}\rvert^2 < 1.3 \times 10^{-4}$

Table 3. Limits on Y couplings coming from upper bounds on $\tau \to P\ell$ branching fractions, determined at the B-factories and compiled by [23].

decay modes are always less sensitive to the relevant Y entries compared to the rare leptonic $K_{L,S} \to \ell^+\ell'^-$ modes [21].

3.2.6 LFV semileptonic τ decays

These decays constitute important observables, uniquely sensitive to the third row of Y. Upper limits on their branching fractions have been set by the Belle and BaBar experiments. The width of the pionic channel reads

$$\Gamma_{\tau\to\ell\pi^0} = \frac{|Y_{\ell d}Y^*_{\tau d}|^2}{2048\pi}\frac{f_\pi^2 m_\tau^3}{m_\Delta^4}\left[1 - 3\hat{m}_\ell^2 - 2\hat{m}_\pi^2\right] , \tag{3.24}$$

where we have kept the leading powers of final state particle masses. Decay width for a channel with K_S in the final state is obtained from (3.24) by replacing $Y_{\ell d}Y^*_{\tau d} \to Y_{\ell d}Y^*_{\tau s} - Y_{\ell s}Y^*_{\tau d}$, $f_\pi \to \sqrt{2}f_K$, and $\hat{m}_\pi \to \hat{m}_K$. For the decay channel $\tau \to \mu\eta$ we include amplitudes for both $s\bar{s}$ and $d\bar{d}$ components of η by replacing in eq. (3.24) $|Y_{\ell d}Y^*_{\tau d}|^2 f_\pi^2 \to \left|f_\eta^q Y_{\mu d}Y^*_{\tau d} + \sqrt{2}f_\eta^s Y_{\mu s}Y^*_{\tau s}\right|^2$, where $f_\eta^{q,s}$ are the decay constants of η through $(\bar{d}\gamma^\mu\gamma_5 d + \bar{u}\gamma^\mu\gamma_5 u)/\sqrt{2}$ and $\bar{s}\gamma^\mu\gamma_5 s$ operators, respectively. Following [41], we include the effects of $\eta - \eta'$ mixing by using $f_\eta^q = f_q \cos\phi$ and $f_\eta^s = -f_s \sin\phi$ with phenomenologically viable numerical values of $f_q = 1.07 f_\pi$, $f_s = 1.34 f_\pi$, and $\phi = 39.3°$. With remaining numerical values $f_\pi = 130.4\,\text{MeV}$ [42], $f_K = 156\,\text{MeV}$ [27], and the relevant 90 % C.L. upper bounds on the branching fractions [23] we find a set of constraints shown in table 3.

3.2.7 $\mu - e$ conversion in nuclei

Four fermion effective Lagrangian (3.4) contains also the LFV terms $(\bar{d}\gamma_\mu P_R d)\{\bar{\mu}\gamma^\mu P_R e, \bar{e}\gamma^\mu P_R \mu\}$. The most stringent bound on such interactions is expected from experimental searches for $\mu - e$ conversion in nuclei. In order to derive the relevant constraints one needs to calculate the appropriate nuclear matrix elements of the above operators. A detailed analysis has been carried out in [43]. We can write the nuclear $\mu - e$ conversion rate as

$$\Gamma_{\text{conversion}} = \frac{|Y_{ed}Y^*_{\mu d}|^2}{4m_\Delta^4}|V^{(p)} + 2V^{(n)}|^2 , \tag{3.25}$$

JHEP11(2011)002

Nucleus	$V^{(p)}[m_\mu^{(5/2)}]$	$V^{(n)}[m_\mu^{(5/2)}]$	$\Gamma_{\text{capture}}[10^6 s^{-1}]$
Ti_{22}^{48}	0.0396	0.0468	2.59
Au_{79}^{197}	0.0974	0.146	13.07

Table 4. Data taken from tables I and VIII of [43].

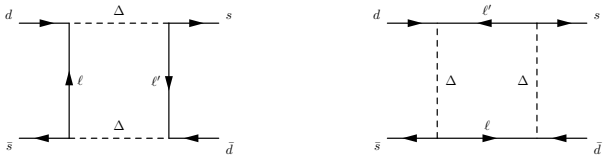

Figure 1. $K - \bar{K}$ mixing diagrams with leptons and Δ in the box loop.

where the nuclear matrix elements $V^{(p,n)}$, calculated in [43] for titanium and gold nuclei are given in table 4. Presently the most stringent bounds on $\mathcal{B}_{\mu e} \equiv \Gamma_{\text{conversion}}/\Gamma_{\text{capture}}$ was set by the SINDRUM collaboration with $\mathcal{B}_{\mu e}^{(\text{Ti})} < 4.3 \times 10^{-12}$ [44] and $\mathcal{B}_{\mu e}^{(\text{Au})} < 7 \times 10^{-13}$ [45], both at 90 % C.L.. Comparing these with our theoretical expressions we obtain the corresponding $1\,\sigma$ bounds

$$|Y_{ed} Y_{\mu d}^*|^2 < 1.9(20) \times 10^{-13} \left(\frac{m_\Delta}{400\ \text{GeV}}\right)^4 \quad \text{from Au(Ti)}\,. \tag{3.26}$$

Note that the same couplings also appear in the $\pi^0 \to e^\pm \mu^\mp$ decay branching fraction, whose expectation is thus pushed far below the current experimental upper bound of $\sim 10^{-10}$.

3.3 One-loop effects of Δ

Next we turn our attention to observables which are affected by leptoquark couplings of Δ at the one-loop level. These are $K - \bar{K}$ and $B - \bar{B}$ mixing amplitudes, LFV neutral current processes like the radiative μ and τ decays, as well as flavor diagonal observables, such as the anomalous magnetic moments of leptons or the decay width of the Z to $b\bar{b}$ pairs. With the exploratory nature of our study in mind, we do not consider nonlocal loop contributions due to the effective four-fermion Lagrangian (3.4), since such effects are constrained by the tree-level processes already considered in section 3.2. The particular case of new absorptive contributions affecting $B_s - \bar{B}_s$ oscillations will be discussed in section 4.

3.3.1 ϵ_K and Δm_K

The SM result for the dispersive mixing matrix element, relevant for ϵ_K is [46]

$$M_{12K}^{\text{SM}} = \frac{G_F^2 m_W^2}{12\pi^2} f_K^2 m_K \hat{B}_K \left[\lambda_c^2 \eta_1 S_0(x_c) + \lambda_t^2 \eta_2 S_0(x_t) + 2\lambda_c \lambda_t \eta_3 S_0(x_c, x_t)\right]\,. \tag{3.27}$$

S_0 is the Inami-Lim box loop function [47] and factors $\lambda_i = V_{is} V_{id}^*$ are the appropriate CKM weights. Explicit λ_u contributions are eliminated using the Glashow-Iliopoulos-Maiani mechanism. Parameters η_1, η_2, and η_3 account for the QCD renormalization effects

JHEP11(2011)002

$\lvert\epsilon_K\rvert$	$2.228(11) \times 10^{-3}$	[23]
Δm_K	$3.483(6) \times 10^{-15}\,\text{GeV}$	[23]
ϕ_ϵ	$43.5(7)^\circ$	[23]
f_K	$0.1560(11)\,\text{GeV}$	[27]
$\hat{B}_K$	0.725(26)	[27]
κ_ϵ	0.94(2)	[48]
η_1	$1.31(^{+25}_{-22})$	[49]
η_2	0.57(1)	[46, 50]
η_3	0.496(47)	[51]

Table 5. Experimental, nonperturbative, and perturbative parameters relevant for ϵ_K and Δm_K observables.

and are known to NLO ($\eta_{1,2}$) or NNLO (η_3) order. The decay constant f_K and the reduced bag parameter $\hat{B}_K$, both nonperturbative QCD parameters, are provided by lattice QCD calculations. Values of all the relevant experimental as well as theoretical parameters are compiled, together with their uncertainties, in table 5. The $K - \bar{K}$ transition is mediated also by box diagrams involving the Δ and leptons, as shown in figure 1, that generate an additional right-handed current operator in the effective Hamiltonian [52]

$$\mathcal{H}^{\Delta}_{\Delta S=2} = \frac{1}{128\pi^2 m_\Delta^2}\left[\sum_\ell Y_{\ell d} Y^*_{\ell s}\right]^2 (\bar{d}_R\gamma^\mu s_R)(\bar{d}_R\gamma_\mu s_R)\,. \tag{3.28}$$

The dispersive mixing matrix element M_{12K} induced by Δ is therefore

$$M^{\Delta}_{12K} = \frac{1}{384\pi^2 m_\Delta^2} f_K^2 m_K \hat{B}_K \eta_2 \left[\sum_\ell Y_{\ell d} Y^*_{\ell s}\right]^2, \tag{3.29}$$

where we have neglected the small QCD running effects from the Δ mass scale to the EW scale and simply use η_2 to describe the renormalization group evolution of Δ contributions down to the hadronic scale. The observable measuring the CP-even component of the K_L mass-eigenstate, ϵ_K, is defined as the ratio of isospin singlet amplitudes of $K_{S(L)} \to \pi\pi$ decays

$$\epsilon_K \equiv \frac{A(K_L \to (\pi\pi)_{I=0})}{A(K_S \to (\pi\pi)_{I=0})}\,, \tag{3.30}$$

and is related to the imaginary part of the dispersive mixing amplitude as [48]

$$\epsilon_K = \kappa_\epsilon \frac{e^{i\phi_\epsilon}}{\sqrt{2}} \frac{\text{Im} M_{12K}}{\Delta m_K}\,. \tag{3.31}$$

Here Δm_K is the measured mass difference between K_L and K_S eigenstates, while ϕ_ϵ is the superweak phase, given by $\phi_\epsilon = \arctan(2\Delta m_K/\Delta\Gamma_K)$. The overall factor κ_ϵ contains long distance corrections and uncertainties [48]. The resulting constraint on the Y couplings is

JHEP11(2011)002

then

$$\left|G_F^2 m_W^2 \mathrm{Im}\left[\lambda_c^2 \eta_1 S_0(x_c) + \lambda_t^2 \eta_2 S_0(x_t) + 2\lambda_c\lambda_t \eta_3 S_0(x_c, x_t)\right] + \frac{\eta_2}{16 m_\Delta^2} \mathrm{Re}\left[\sum_\ell Y_{\ell d} Y_{\ell s}^*\right] \mathrm{Im}\left[\sum_\ell Y_{\ell d} Y_{\ell s}^*\right]\right|$$
$$= \frac{12\sqrt{2}\pi^2}{f_K^2 \hat{B}_K \kappa_\epsilon} \frac{\Delta m_K}{m_K} |\epsilon_K| = 1.57(7) \times 10^{-13}\ \mathrm{GeV}^{-2}\,, \tag{3.32}$$

where on the right-hand side, we have combined the experimental and theoretical (hadronic) uncertainties by summing them in squares. Nonetheless, some theoretical uncertainty coming from the QCD renormalization factors $\eta_{1,2,3}$ still remains on the left-hand side. In the fit we allow them to freely vary within the intervals determined by their theoretical uncertainties (see table 5).

The measured mass difference Δm_K, on the other hand, mostly probes the real part of the mixing amplitude M_{12K} [53]. It receives potentially important contributions from SM long distance dynamics leading to large theoretical uncertainties in its prediction [49]. Therefore we conservatively assume that the short distance contribution of M_{12K}^Δ must be smaller than half the experimental value of Δm_K at $1\,\sigma$ C.L.:

$$\Delta m_K^\Delta \simeq \mathrm{Re}\, M_{12K}^\Delta = \frac{1}{192\pi^2 m_\Delta^2} f_K^2 m_K \hat{B}_K \eta_2 \mathrm{Re}\left[\sum_\ell Y_{\ell d} Y_{\ell s}^*\right]^2 < 1.74 \times 10^{-15}\ \mathrm{GeV}\,. \tag{3.33}$$

The conservative assumption for the bound (3.33) allows us to neglect uncertainties of all the theoretical parameters and extract the following $1\,\sigma$ bound on the real part of the Y combination

$$\mathrm{Re}\left[\sum_\ell Y_{\ell d} Y_{\ell s}^*\right]^2 < 1.1 \times 10^{-4} \left(\frac{m_\Delta}{400\ \mathrm{GeV}}\right)^2\,. \tag{3.34}$$

3.3.2 $B_d - \bar{B}_d$ and $B_s - \bar{B}_s$ mixing

The time evolution of the $B - \bar{B}$ system is described by the average mass m, width Γ, and three mixing parameters

$$|M_{12}|, \qquad |\Gamma_{12}|, \qquad \phi = -\arg(M_{12}/\Gamma_{12})\,. \tag{3.35}$$

All five parameters can be identified by diagonalizing the effective Hamiltonian

$$H_{\mathrm{eff}} = M - \frac{i}{2}\Gamma = \begin{pmatrix} m & M_{12} \\ M_{12}^* & m \end{pmatrix} - \frac{i}{2}\begin{pmatrix} \Gamma & \Gamma_{12} \\ \Gamma_{12}^* & \Gamma \end{pmatrix}\,, \tag{3.36}$$

whose off-diagonal elements are defined as $(H_{\mathrm{eff}})_{12} = \left\langle B \left| \mathcal{H}_{\mathrm{eff}}^{\Delta B=2} + \text{nonlocal interactions} \right| \bar{B} \right\rangle / (2m)$ and Γ_{12} contains all on-shell contributions of intermediate poles. Heavy and light (H and L) mass-eigenstates are defined as

$$|B_{H,L}\rangle = p\,|B\rangle \pm q\,|\bar{B}\rangle\,, \tag{3.37}$$

and their eigenvalues are, in the appropriate limit $|\Gamma_{12}| \ll |M_{12}|$, in turn connected to the measurements of Δm and $\Delta\Gamma$ as

$$\Delta m \equiv m_H - m_L = 2|M_{12}|\,, \tag{3.38a}$$
$$\Delta\Gamma \equiv \Gamma_L - \Gamma_H = 2|\Gamma_{12}|\cos\phi\,. \tag{3.38b}$$

JHEP11(2011)002

$\sin 2\beta$	0.673(23)	[54]
Δm_d	0.507(5) ps^{-1}	[23]
Δm_s	17.77(12) ps^{-1}	[23]
$f_{B_s}(\hat{B}_{B_s})^{1/2}$	0.275(15) GeV	[27]
ξ	1.237(32)	[27]
η_B	0.55(1)	[46, 56]

Table 6. Experimental, nonperturbative, and perturbative parameters relevant for $B_{d(s)} - \bar{B}_{d(s)}$ mixing.

If CP violation in decays is negligible, one can extract the phase ϕ from the semileptonic time-dependent CP asymmetry

$$a_{\rm sl}(t) = \frac{\Gamma(\bar{B}(t) \to \ell^+ X) - \Gamma(B(t) \to \ell^- X)}{\Gamma(\bar{B}(t) \to \ell^+ X) + \Gamma(B(t) \to \ell^- X)} = \frac{\Delta\Gamma}{\Delta m} \tan\phi \ . \tag{3.39}$$

The overall $\Delta\Gamma/\Delta m$ factor renders this asymmetry very small. Measurements of $a_{\rm sl}^{(d)}$ in the B_d system have been performed at the B-factories and a world average [54] is consistent with zero, albeit with much larger errors than the SM predicted value. Direct measurement of $a_{\rm sl}^{(s)}$ is not available, however DØ and CDF experiments [54] have measured the charge asymmetry of same-charge dimuon events coming from inclusive b-decays, which is a linear combination of $a_{\rm sl}^{(d)}$ and $a_{\rm sl}^{(s)}$, thus allowing one to extract $a_{\rm sl}^{(s)}$. Especially the DØ measurements [13, 16, 17] point at an unexpectedly large mixing phase ϕ and exclude the SM value of $a_{\rm sl}^{(s)}$ with more than $3\,\sigma$ significance [18, 19, 55].

More effectively, one can extract the phase in the dispersive mixing amplitude M_{12} from the time-dependent CP asymmetry in decays of B ($\bar{B}$) to CP eigenstates

$$A_{\rm CP}^f(t) = \frac{\Gamma(B(t) \to f) - \Gamma(\bar{B}(t) \to f)}{\Gamma(B(t) \to f) + \Gamma(\bar{B}(t) \to f)} = \eta_f {\rm Im}\left(\frac{p}{q}\right) \sin\Delta m\, t\,, \tag{3.40}$$

where we have assumed a tree-level dominated decay mechanism, negligible CP violation in the decay, and also $|p/q| = 1$. CP parity of the final state is denoted as η_f. To leading order in $|\Gamma_{12}/M_{12}|$, Γ_{12} cancels out and one is sensitive to the phase of M_{12} through ${\rm Im}(p/q) = {\rm Im}(M_{12})/|M_{12}|$. This phase is interpreted within the SM as an angle of the unitarity triangle $\sin 2\beta$ ($\sin 2\beta_s$) in the case of the B_d (B_s) system. Note that the weak phase of the absorptive part is negligible in the SM and also difficult to enhance in most NP scenarios and thus $\phi_{d(s)} \approx -2\beta_{(s)}$ (we will comment on the recent study [52] of Δ contributions to the absorptive amplitude in section 4).

At this point we shall include as experimental constraints only the measurements of $\sin 2\beta$ and the mass splittings Δm_d, Δm_s. We will address the allowed ranges of ϕ_s in the fit part in section 4. The SM prediction for the dispersive matrix element M_{12} in B_d mixing (with obvious replacements in the case of B_s mixing), is dominated by the short distance box diagrams involving the top quark

$$M_{12B}^{\rm SM} = \frac{G_F^2 m_W^2}{12\pi^2} f_B^2 m_B \hat{B}_B (V_{tb}V_{td}^*)^2 \eta_B S_0(x_t)\,. \tag{3.41}$$

JHEP11(2011)002

The three theoretical parameters here are again the perturbative QCD renormalization factor η_B, and the nonperturbative hadronic parameters f_B and $\hat{B}_B$. Box diagrams with Δ, analogous to the ones of $K-\bar{K}$ in figure 1, can shift the value of $M_{12}^{\rm SM}$ by

$$M_{12B}^{\Delta} = \frac{1}{384\pi^2 m_\Delta^2} f_B^2 m_B \hat{B}_B \eta_B \left[\sum_\ell Y_{\ell d} Y_{\ell b}^*\right]^2 , \tag{3.42}$$

where we again neglect the difference between the Δ and EW matching scales. Instead of using Δm_d and Δm_s as individual fit constraints, we opt to trade Δm_d for the ratio $\Delta m_s/\Delta m_d$ depending on the hadronic parameter $\xi(\equiv \hat{B}_{B_s}\sqrt{f_{B_s}}/\hat{B}_{B_d}\sqrt{f_{B_d}})$ that can be determined reliably using lattice QCD techniques

$$\left|\frac{(V_{tb}V_{ts}^*)^2 S_0(x_t) + (32 m_\Delta^2 G_F^2 m_W^2)^{-1} \left(\sum_\ell Y_{\ell s} Y_{\ell b}^*\right)^2}{(V_{tb}V_{td}^*)^2 S_0(x_t) + (32 m_\Delta^2 G_F^2 m_W^2)^{-1} \left(\sum_\ell Y_{\ell d} Y_{\ell b}^*\right)^2}\right| = \frac{\Delta m_s}{\Delta m_d}\frac{m_{B_d}}{m_{B_s}}\xi^{-2} = 22.5(12)\,, \tag{3.43a}$$

$$\left|(V_{tb}V_{ts}^*)^2 S_0(x_t) + (32 m_\Delta^2 G_F^2 m_W^2)^{-1}\left[\sum_\ell Y_{\ell s} Y_{\ell b}^*\right]^2\right| = \Delta m_s \frac{6\pi^2}{G_F^2 m_W^2 \eta_B \hat{B}_{B_s} f_{B_s}^2 m_{B_s}} = 3.53(39)\times 10^{-3}\,. \tag{3.43b}$$

On the right-hand sides, we have combined the experimental and theoretical errors in quadrature. The relevant numerical inputs are compiled in table 6. On the other hand, in the $\sin 2\beta$ constraint all dependence on theoretical (in particular hadronic) parameters drops out

$$\frac{{\rm Im}\left[S_0(x_t)(V_{tb}V_{td}^*)^2 + (32 m_\Delta^2 G_F^2 m_W^2)^{-1}\left(\sum_\ell Y_{\ell d} Y_{\ell b}^*\right)^2\right]}{\left|S_0(x_t)(V_{tb}V_{td}^*)^2 + (32 m_\Delta^2 G_F^2 m_W^2)^{-1}\left(\sum_\ell Y_{\ell d} Y_{\ell b}^*\right)^2\right|} = \sin 2\beta\,. \tag{3.44}$$

3.3.3 Anomalous magnetic and electric dipole moments

The electromagnetic interactions of an on-shell fermion can be parameterized in terms of parity conserving and parity violating form factors [57]

$$\mathcal{A}^\mu \equiv -ie\bar{u}(p',s')\Gamma^\mu u(p,s), \tag{3.45a}$$

$$\Gamma^\mu = F_1\gamma^\mu + \frac{F_2}{2m_\mu} i\sigma^{\mu\nu}q_\nu + F_3\sigma^{\mu\nu}q_\nu\gamma_5 + F_4(2mq^\mu + q^2\gamma^\mu)\gamma_5\,, \tag{3.45b}$$

where $q = p - p'$. This is the most general form of the photon off-shell amplitude obeying the Ward identity of quantum electrodynamics

$$q_\mu \mathcal{A}^\mu = 0\,. \tag{3.46}$$

Renormalized charge of a muon is $-e$ and so $F_1(0) = 1$ exactly. A finite $F_3(0)$ would signal a nonzero electric dipole moment in presence of CP violating phases in the renormalized vertex. $F_4(0)$ is called the anapole moment. The form factor F_2, which is the source of the anomalous magnetic moment, enters in the gyromagnetic ratio as $g = 2(F_1(0) + F_2(0))$. Comparing precise measurements of these form factors against theoretical higher-order predictions presents powerful tests of the SM and its extensions. In the recent years, the

Figure 2. Diagrams with Δ and down-quarks contributing to the lepton anomalous magnetic moments.

experimental result on the anomalous magnetic moment of the muon $a_\mu \equiv (g-2)_\mu/2$ from BNL [10] has been about $3\,\sigma$ above theoretical predictions within the SM [11]

$$a_\mu^{\rm exp} = 1.16592080(63) \times 10^{-3}\,, \tag{3.47a}$$
$$a_\mu^{\rm SM} = 1.16591793(68) \times 10^{-3}\,. \tag{3.47b}$$

Treating both experimental and theoretical uncertainties as Gaussian, we may identify the missing contribution to a_μ

$$\delta a_\mu = a_\mu^{\rm exp} - a_\mu^{\rm SM} = (2.87 \pm 0.93) \times 10^{-9}\,, \tag{3.48}$$

with the presence of NP. The leading Δ contributions to a_μ with Δ and down quarks d_i running in the loop (figure 2) are expected to be of the order $\sim 1/(4\pi)^2\, m_\mu^2/m_\Delta^2\, e|Y_{\mu i}|^2$ and have been previously computed in [58]. We reproduce the magnitude of a_μ of [58], however with an opposite overall sign

$$a_\mu = \frac{3m_\mu^2}{16\pi^2 m_\Delta^2} \sum_{i=d,s,b} |Y_{\mu i}|^2 \left[Q_\Delta f_\Delta(x_i) + Q_d f_d(x_i)\right], \qquad x_i = m_{d_i}^2/m_\Delta^2. \tag{3.49}$$

Here the charges are $Q_{\Delta,d} = 4/3,\ -1/3$ while $f_{\Delta,d}$ are the loop functions

$$f_\Delta(x) = \frac{2x^3 + 3x^2 - 6x^2\log x - 6x + 1}{6(x-1)^4}\,, \tag{3.50a}$$
$$f_d(x) = \frac{-x^3 + 6x^2 - 6x\log x - 3x - 2}{6(x-1)^4}\,. \tag{3.50b}$$

In the limit $x_i \to 0$ the result becomes

$$a_\mu = \frac{3m_\mu^2(Q_\Delta - 2Q_d)}{96\pi^2 m_\Delta^2} \sum_{i=d,s,b} |Y_{\mu i}|^2 = \frac{1}{16\pi^2}\frac{m_\mu^2}{m_\Delta^2} \sum_{i=d,s,b} |Y_{\mu i}|^2. \tag{3.51}$$

If we now saturate δa_μ with a_μ we find that a non-zero magnitude is preferred for a combination of the second row elements of Y

$$\sum_{i=d,s,b} |Y_{\mu i}|^2 = (4.53 \pm 1.47) \times 10^{-7} \times \frac{m_\Delta^2}{m_\mu^2} = (6.45 \pm 2.09) \times \frac{m_\Delta^2}{(400\ {\rm GeV})^2}\,. \tag{3.52}$$

We will further explore the possible correlations of such effects with other constraints in section 4.

JHEP11(2011)002

decay mode	90 % C.L. exp. bound on $\mathcal{B}$	$1\,\sigma$ upper bound in units $(m_\Delta/400\text{ GeV})^4$
$\mu \to e\gamma$	2.4×10^{-12}	$\lvert\sum_{i=d,s,b} Y_{ei}Y^*_{\mu i}\rvert^2 < 4.6 \times 10^{-8}$
$\tau \to \mu\gamma$	4.4×10^{-8}	$\lvert\sum_{i=d,s,b} Y_{\mu i}Y^*_{\tau i}\rvert^2 < 4.8 \times 10^{-3}$
$\tau \to e\gamma$	3.3×10^{-8}	$\lvert\sum_{i=d,s,b} Y_{ei}Y^*_{\tau i}\rvert^2 < 3.6 \times 10^{-3}$

Table 7. Limits on Y couplings coming from upper bounds of LFV radiative lepton decay branching fractions, taken from [23, 59].

On the other hand, applying expression (3.52) to the electron case and requiring that a_e^Δ be smaller than the experimental uncertainty, we find a $1\,\sigma$ bound on the first row of Y

$$\sum_{i=d,s,b} |Y_{ei}|^2 < 8.8 \times 10^{-11} \times \frac{m_\Delta^2}{m_e^2} = 54 \times \frac{m_\Delta^2}{(400\text{ GeV})^2}\,, \tag{3.53}$$

where we have used the experimental uncertainty estimate of $\sigma_{a_e}^{\text{exp}} = 2.8 \times 10^{-13}$ [23].

Finally, we note that due to the Hermitian structure of Y contributions to the EM interactions of quarks and leptons, no electric (or chromoelectric) dipole moments of either quarks or leptons are generated at the one loop level, regardless of the phases present in Y. Furthermore, even at the two loop level, non-zero contributions can only originate from mixed $W - \Delta$ loops. However, since Δ interactions are purely right-handed, such contributions are necessarily suppressed both by CKM factors and by insertions of the light quark or lepton masses. Therefore we do not consider them further.

3.3.4 Flavor violating radiative decays

The computation of Δ contributions to the LFV radiative muon decay is analogous to the magnetic moment diagrams in figure 2 and results in the effective Lagrangian

$$\mathcal{L}^\Delta_{\mu\to e\gamma} = \frac{e}{64\pi^2 m_\Delta^2}\left[\sum_{i=d,s,b} Y_{ei}Y^*_{\mu i}\right]\bar{e}(\sigma^{\mu\nu}F_{\mu\nu})(m_\mu P_L + m_e P_R)\mu\,. \tag{3.54}$$

The decay width of $\mu \to e\gamma$ is then given by

$$\Gamma_{\mu\to e\gamma} = \frac{\alpha m_\mu^5}{4096\pi^4 m_\Delta^4}\left|\sum_{i=d,s,b} Y_{ei}Y^*_{\mu i}\right|^2. \tag{3.55}$$

The above expression can also be applied to the LFV decays of the τ, with obvious replacements in Y indices and masses. Inequalities following from upper limits on branching fractions of $\ell \to \ell'\gamma$ are shown in table 7. Consequently, measurements of these flagship LFV processes impose strict requirements on the structure of Y, namely they require that rows of Y are approximately orthogonal.

On the other hand, the analogous constraints coming from the quark sector radiative decays are much weaker. The prominent example of $b \to s\gamma$ has recently been analyzed in [55], where it was found that this decay is not very sensitive to the relevant Δ interactions, which contribute at one loop through the insertion of the Lagrangian (3.4). In particular, the Δm_s constraint (3.43b) yields consistently stronger bounds on the same combination of Y elements for the experimentally allowed range of Δ masses.

JHEP11(2011)002

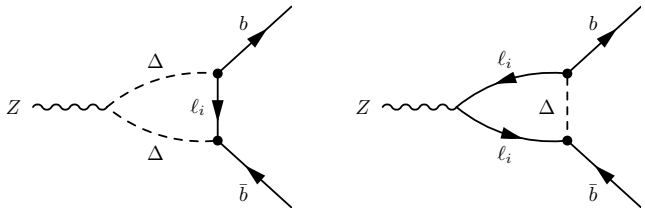

Figure 3. Diagrams with Δ and leptons modifying the $Zb\bar{b}$ vertex.

3.3.5 Decay width of $Z \to b\bar{b}$

The experiments running on the LEP 1 collider performed precise measurements of the relative widths of $Z \to b\bar{b}$ and $Z \to$ hadrons. In particular the experimental value of

$$R_b = \frac{\Gamma(Z \to b\bar{b})}{\Gamma(Z \to \text{hadrons})}\,, \tag{3.56}$$

is according to the PDG [23] in good agreement with SM predicted value

$$R_b^{\text{exp}} = 0.21629(66)\,, \tag{3.57a}$$
$$R_b^{\text{SM}} = 0.21578(5)\,. \tag{3.57b}$$

The SM tree-level amplitude for the $Zb\bar{b}$ vertex is

$$\mathcal{A}^{\text{tree}} = \mathrm{i}g_Z\Big[g_R^0\mathcal{A}_R + g_L^0\mathcal{A}_L\Big]\,, \qquad \mathcal{A}_{L(R)} = Z_\mu\,\bar{b}\gamma_\mu P_{L(R)}b\,, \tag{3.58}$$
$$g_R^0 = \frac{1}{3}\sin^2\theta_W\,, \qquad g_L^0 = -1/2 + \frac{1}{3}\sin^2\theta_W\,,$$

where $g_Z = g/\cos\theta_W$. New contributions of Δ change g_R^0 to $g_R = g_R^0 + \delta g_R$, where

$$\delta g_R = \sin^2\theta_W \frac{\sum_\ell |Y_{\ell b}|^2}{(4\pi)^2}\frac{1}{6x_Z^2}\left[\frac{17}{2}x_Z^2 - 2x_Z + \log(x_Z)\big(3x_Z^2 - 6x_Z + 6\log(1+x_Z)\big)\right. \tag{3.59}$$
$$\left. -8f_1 + 4f_2(2x_Z - x_Z^2) + 6\mathrm{Li}_2(-x_Z) - \mathrm{i}\pi\Big(3x_Z^2 - 6x_Z + 6\log(1+x_Z)\Big)\right]\,,$$

and $x_Z = m_Z^2/m_\Delta^2$. Calculational details along with functions f_1 and f_2 are given in the appendix A. Taking into account higher order SM corrections, the relative shift in R_b due to such NP contributions can be written as [60]

$$\delta R_b = 2R_b^{\text{SM}}(1 - R_b^{\text{SM}})\frac{g_L^0\,\text{Re}(\delta g_L) + g_R^0\,\text{Re}(\delta g_R)}{(g_L^0)^2 + (g_R^0)^2}\,. \tag{3.60}$$

One can check that the shift $\text{Re}(\delta g_R)$ given in eq. (3.59) is negative and $\delta g_L = 0$ and consequently any contributions of Δ necessarily worsen the agreement between theory and experiment. If the discrepancy should be smaller than $1\,\sigma$ the following constraint has to be met

$$\sum_\ell |Y_{\ell b}|^2 < 5.60\left(\frac{m_\Delta}{400\text{ GeV}}\right)^2 + 6.73\left(\frac{m_\Delta}{400\text{ GeV}}\right) + 2.02\,. \tag{3.61}$$

JHEP11(2011)002

In derivation of this bound we have approximated δg_R by a polynomial in variable m_Δ and employed $\sin^2\theta_W = 0.231$ [23].

On the other hand, the forward-backward asymmetry in $b\bar{b}$ production as measured at LEP exhibits a $2.7\,\sigma$ tension with the SM EW fit. Since Δ contributions only affect the right-handed effective $Zb\bar{b}$ coupling (δg_R) they cannot fully reconcile this tension [60] and we do not include this observable in the fit.

4 Global fit of the leptoquark couplings

In this section we perform a global fit of Y to all the observables listed in section 3, while we keep fixed $m_\Delta = 400\,\text{GeV}$. We resort to a $\chi^2(Y)$ statistic that we minimize to find the point $\chi^2_{\text{min}} = \chi^2(Y_{\text{best}})$, where Y is by definition in best agreement with all the constraints. $\chi^2(Y)$ is written as a sum of Gaussian contributions of observables $\mathcal{O}_i$

$$\chi^2(Y) = \sum_i \frac{\left(\mathcal{O}_i^{\text{exp}} - \mathcal{O}_i^{\text{prediction}}(Y)\right)^2}{\left(\sigma_i^{\text{eff}}\right)^2}\,. \tag{4.1}$$

Values of $\mathcal{O}_i^{\text{exp}}$ and σ_i^{eff} are central values and errors, read-off from right-hand sides of constraining equations in the preceding sections, whereas $\mathcal{O}_i^{\text{prediction}}$ are the corresponding predictions in terms of Y_{ij}, i.e., the left-hand sides of constraints, in the language of section 3. Majority of $\mathcal{O}_i^{\text{exp}}$ are upper bounds which are modeled with χ^2 centered at zero. This is achieved in eq. (4.1) by setting $\mathcal{O}_i^{\text{exp}} = 0$ and σ_i^{eff} to the derived 68 % C.L. upper bound. Although not explicitly shown here, the χ^2 function (4.1) depends also on the 4 Wolfenstein parameters of the CKM matrix (they are present in meson mixing constraints) and we treat them on the same footing as Y. We add to (4.1) a Gaussian chi-square term which guides the CKM parameters to follow probability distribution of eqs. (3.2) and (3.3).

Statistical interpretation of the value of χ^2, i.e. the goodness of fit, is performed using the standard χ^2 probability distribution with appropriate number of degrees of freedom, $N_{\text{DOF}} = N_{\text{observables}} - N_{\text{parameters}} = 36 - 21$. To find the allowed range of a single matrix element $|Y_{ij}|$, its phase, or a function of several Y elements, denoted in the following generically as $z(Y)$, we minimize χ^2 with $z(Y)$ fixed to some chosen value z_0. Then all values z_0, where

$$\min\left[\chi^2(Y)_{z(Y)=z_0}\right] - \chi^2_{\text{min}} < 1\,(4) \tag{4.2}$$

form the 68.3 (95.45) % C.L. interval for the parameter z. To find confidence level regions in two-dimensional scans (with two fixed quantities $z(Y)$, $w(Y)$) we utilize the χ^2-distribution with 2 degrees of freedom. The difference $\Delta\chi^2(z_0, w_0) = \min[\chi^2_{z(Y)=z_0, w(Y)=w_0}] - \chi^2_{\text{min}}$ for points (z_0, w_0) in the $N\,\sigma$ C.L. region in this case is

$$1 - \exp\left[-\Delta\chi^2(z_0, w_0)/2\right] < \text{erf}\left(\frac{N}{\sqrt{2}}\right)\,. \tag{4.3}$$

4.1 Structure of Y

In a trivial case, when we set $Y = 0$ to recover the SM, we find $\chi^2_{\text{min}} = 12.5 = 9.5_{a_\mu} + 1.5_{\text{CKM}} + 0.8_{\Delta m_s} + \cdots$ with a dominant contribution from the a_μ anomaly. If we let

JHEP11(2011)002

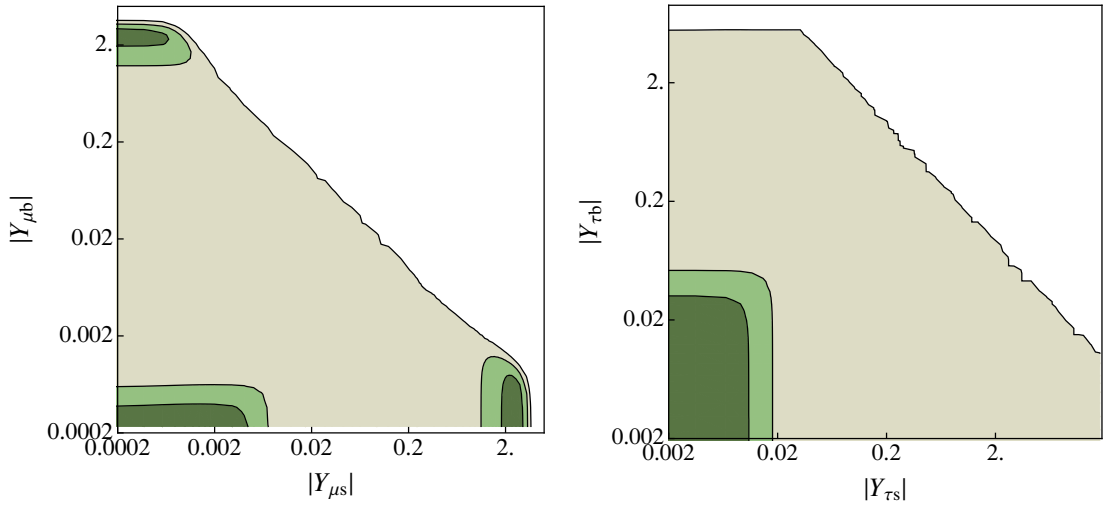

Figure 4. Correlation between elements in the second ($|Y_{\mu s}|$ and $|Y_{\mu b}|$) and third ($|Y_{\tau s}|$ and $|Y_{\tau b}|$) row. Dark green region is the $1\,\sigma$ contour, while the two lighter green contours are 2 and $3\,\sigma$, respectively.

Y take any value we find a global minimum $\chi^2_{\rm min} = 2.5 = 1.8_{\rm CKM} + 0.4_{\Delta m_s} + \cdots$ for 15 degrees of freedom, which signals a very good agreement of all predictions with the considered observables. In particular, the best point perfectly resolves the anomalous magnetic moment constraint a_μ and slightly improves quark flavor constraints. The allowed 1 and $2\,\sigma$ ranges of Y matrix elements are shown below

$$|Y^{(1\,\sigma)}| \in \begin{pmatrix} < 1.4\times10^{-6} & < 8.7\times10^{-5} & < 4.1\times10^{-4} \\ < 3.6\times10^{-3}\cup[2.1,2.9] & < 3.6\times10^{-3}\cup[2.1,2.9] & < 6.2\times10^{-4}\cup[2.3,2.7] \\ < 5.6\times10^{-3} & < 8.1\times10^{-3} & < 9.6\times10^{-3} \end{pmatrix}, \tag{4.4a}$$

$$|Y^{(2\,\sigma)}| \in \begin{pmatrix} < 2.2\times10^{-6} & < 1.4\times10^{-4} & < 6.6\times10^{-4} \\ < 5.6\times10^{-3}\cup[1.5,3.3] & < 5.6\times10^{-3}\cup[1.5,3.3] & < 9.7\times10^{-4}\cup[1.6,3.2] \\ < 8.9\times10^{-3} & < 1.4\times10^{-2} & < 1.5\times10^{-2} \end{pmatrix}. \tag{4.4b}$$

Couplings to the electron are strongly suppressed, while couplings to the muon (the second row of Y) can take values of order 1, in order to satisfy the a_μ constraint. In the last row, elements $Y_{\tau s}$ and $Y_{\tau b}$ can also be of order 0.01 at $1\,\sigma$ C.L. We find some interesting correlations between the second and third row elements, shown in figures 4 and 5.

We find three distinct regimes in the second and third row (figures 4 and 5), depending on which element in the second row is large. Pictorially, these hierarchies are possible

$$\begin{pmatrix} 0 & 0 & 0 \\ \blacksquare & 0 & 0 \\ \bullet & \bullet & \bullet \end{pmatrix}, \qquad \begin{pmatrix} 0 & 0 & 0 \\ 0 & \blacksquare & 0 \\ \bullet & \bullet & \bullet \end{pmatrix}, \qquad \begin{pmatrix} 0 & 0 & 0 \\ 0 & 0 & \blacksquare \\ \bullet & \bullet & \bullet \end{pmatrix}. \tag{4.5}$$

JHEP11(2011)002

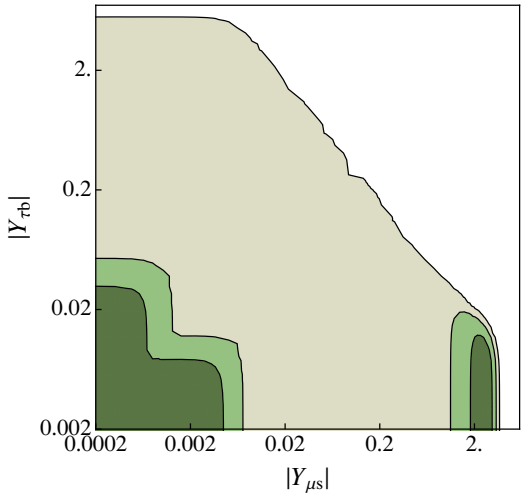

Figure 5. Correlation between diagonal Y elements in the muon and tau rows. Dark green region is the $1\,\sigma$ contour, while the two lighter ones are 2 and $3\,\sigma$, respectively.

Here ■ stands for order 1 element, • for (at most) order 0.01 element, while we neglect elements which are $\lesssim 10^{-3}$. This particular hierarchy is enforced by a nontrivial a_μ constraint that requires at least one large element in the second row, while stringent upper bounds from LFV processes exclude the possibility of having two elements of order 1.

We also identify the observables, which are most constraining for each element in Y. We do this by registering the maximum increase in each individual observable contribution to χ^2 when a single Y element is changed from its best-fit value. In the first row, all the most stringent constraints actually also involve the $Y_{\mu q}$ elements: $K_L \to \mu^\pm e^\mp$ (Y_{ed}), $\mu \to e\gamma$ (Y_{es}) and $B \to \pi\mu^\pm e^\mp$ (Y_{eb}). In the near future, we can expect some significant improvement at least for Y_{es} from the MEG experiment [61, 62]. The best-fit regions around $\mathcal{O}(1)$ values for the second row elements are mostly determined by the observed discrepancy in the a_μ. Other relevant observables, that constrain their values in the $\ll 1$ regions are: Δm_K and $K_S \to \mu^+\mu^-$ $(Y_{\mu d}, Y_{\mu s})$, and $B \to X_s\ell^+\ell^-$ $(Y_{\mu b})$. Unfortunately, due to the theoretical uncertainties which dominate the precision of the first two observables, a significant improvement in the foreseeable future can only be expected for the constraint on $Y_{\mu b}$ from the Super Flavor factories (SFFs) [63, 64]. Finally, the constraints on the third row of Y are dominated by LFV tau and B decays: $\tau \to \mu\pi_0$ and $\tau \to \mu\eta$ $(Y_{\tau d})$, $B \to K\tau^\pm\mu^\mp$ $(Y_{\tau s})$, and $B \to K\tau^\pm\mu^\mp$ and $\tau \to \mu K_S$ $(Y_{\tau b})$. Again SFFs are expected to yield improved bounds on these LFV observables. Finally we note the fact that bounds on most of the elements of Y are dominated by rare decays and the a_μ which all exhibit a similar scaling dependence on the Δ parameters (Y/m_Δ). This points towards an approximate linear scaling of the fitted Y element values with the Δ mass and allows for simple reinterpretation of the derived limits at Δ masses away from the reference value $m_\Delta = 400\,\text{GeV}$.

JHEP11(2011)002

4.2 Comment on tension between $\mathcal{B}(B \to \tau\nu)$ and $\sin 2\beta$

We can redo the tree-level CKM fit, described in section 3.1, replacing the $|V_{ub}|$ value from eq. (3.1) with a constraint coming from a world average of Belle and BaBar measurements [65–68] of $\mathcal{B}(B^+ \to \tau^+\nu) = (1.68 \pm 0.31) \times 10^{-4}$ [19]. The observable cannot be directly affected by Δ contributions and is given in the SM by

$$\mathcal{B}(B^+ \to \tau^+\nu_\tau) = \frac{G_F^2 m_{B^+} m_\tau^2}{8\pi} \left(1 - \frac{m_\tau^2}{m_{B^+}^2}\right)^2 |V_{ub}|^2 f_B^2 \tau_{B^+} \,. \tag{4.6}$$

The main theoretical uncertainty due to the lattice QCD estimate of the relevant decay constant $f_B = 193 \pm 10$ MeV [27] is at present subleading compared to the experimental error, but we nevertheless combine them in quadrature. The best-fitted values of the CKM parameters are then

$$\begin{aligned} \lambda &= 0.22538(65)\,, \\ A &= 0.799(26)\,, \\ \rho &= 0.162(90)\,, \\ \eta &= 0.528(64)\,. \end{aligned} \tag{4.7}$$

The quality of the fit of the CKM from tree-level observables is exactly the same as in section 3.1, however the central values of ρ and especially η are significantly higher than before. This is expected since the tree level fit of ρ and η parameters is not over-constrained. We can also repeat the global fit of couplings Y, this time with a Gaussian chi-square term for the CKM matrix corresponding to eq. (4.7) and the underlying correlation matrix. The best fit point with $\chi^2 = 9.5$ relaxes the tension in the CKM by changing the $B_d - \bar{B}_d$ phase ($\sin 2\beta$) but at the price of not resolving the a_μ anomaly at all. Another, slightly shallower, minimum with $\chi^2 = 10.6$ achieves just the reverse — a_μ is perfectly satisfied while the tension in the CKM persists.

A qualitative explanation goes as follows: a new phase in $B_d - \bar{B}_d$ mixing can be generated by either $Y_{ed}Y_{eb}^*$, $Y_{\mu d}Y_{\mu b}^*$ or $Y_{\tau d}Y_{\tau b}^*$. Large $Y_{ed}Y_{eb}^*$ and $Y_{\mu d}Y_{\mu b}^*$ are ruled out by the strong $B \to \pi\ell^+\ell^-$ constraint. Thus for large enough $Y_{\tau d}Y_{\tau b}^*$ either (i) $Y_{\tau d}$ or (ii) $Y_{\tau b}$ is at least ~ 0.1. In turn we form uncomfortably large products of (i) $Y_{\tau d}Y_{\mu q}$ or (ii) $Y_{\tau b}Y_{\mu q}$ for $q = d, s, b$, where $Y_{\mu q}(\sim 1)$ is large to explain a_μ. First possibility ($q = d$) is incompatible with (i) $\tau \to \pi^0\mu$ or (ii) $B_s \to \tau\mu$ branching ratios, second one with (i) $\tau \to K^0\mu$ or (ii) $B \to K\tau\mu$, and the last one with (i) $B_d \to \tau\mu$ or (ii) $\tau \to \mu\gamma$.

Such worsening of the overall agreement of observables with the model can already be anticipated from eqs. (4.4) which clearly state that large contributions to $B_d - \bar{B}_d$ mixing are disfavoured. On the other hand, if one ignores the a_μ constraint, then this model can sufficiently affect the phase of the $B_d - \bar{B}_d$ mixing amplitude to be consistent with a large $\mathcal{B}(B \to \tau\nu)$.

4.3 Comment on CPV in the B_s system

Next, we address the question whether contributions of Δ can enhance the phase of the dispersive amplitude in the $B_s - \bar{B}_s$ system, or even modify the absorptive part by on-shell charged leptons in box diagrams (figure 1). According to [52], which studied $\tau\tau$

JHEP11(2011)002

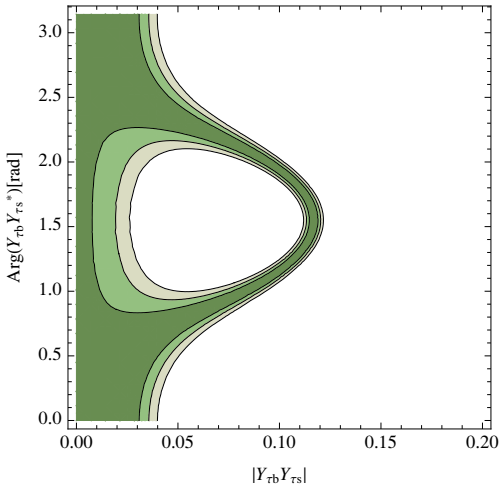

Figure 6. Correlation between the absolute value of $Y_{\tau s}Y^*_{\tau b}$ and its phase ($\mathrm{Arg}(Y_{\tau s}Y^*_{\tau b})$) in absence of the a_μ constraint. Dark green region is the $1\,\sigma$ contour, while the two lighter ones are 2 and $3\,\sigma$, respectively.

absorbtive contributon to mixing amplitude, one should have $Y_{\tau s}Y_{\tau b} \sim 0.1$ for $m_\Delta = 250$ GeV. However, the set of observables we have included in the analysis of Y couplings (in particular a_μ) forces the $\tau\tau$ and $\mu\mu$ states to couple very weakly to B_s

$$|Y_{\mu s}Y^*_{\mu b}| < 0.0015\,(0.0021)\,, \tag{4.8a}$$

$$|Y_{\tau s}Y^*_{\tau b}| < 0.9\times 10^{-4}\,(4.1\times 10^{-4})\,. \tag{4.8b}$$

Bounds are $1\,\sigma\,(2\,\sigma)$ C.L. (see also figure 4) . While $|Y_{\mu s}Y^*_{\mu b}|$ is directly constrained by the $B\to X_s\ell^+\ell^-$ rate, there is presently no direct bound on the magnitude of $Y_{\tau s}Y^*_{\tau b}$, so the constraint (4.8b) is directly linked to the explanation of the a_μ anomaly. Using the above $2\,\sigma$ upper bounds in eq. (3.42) we find that the dispersive Δ amplitude with tau (muon) in the box is five (four) orders of magnitude smaller than the SM contribution.

The approximate scaling of the most important constraints with Y/m_Δ provides a robust bound on the absorptive contributions to the neutral meson mixing amplitudes, excluding any significant modification of $\Delta\Gamma_s$, provided we require the resolution of the a_μ anomaly. We also note in passing that the smallness of new absorptive NP contributions is required in general by the measurements of the lifetime ratios of B mesons, semileptonic branching fractions, and the average number of charm quarks in B decays (see [19] and references therein). On the other hand, the maximum allowed relative Δ contributions to the dispersive parts scale quadratically with m_Δ. In this way dispersive Δ amplitudes comparable in size to SM contributions in $B_s-\bar{B}_s$ mixing observables are only reached at masses well above 1 TeV, where the relevant Y couplings are no longer perturbative. Thus we find no possibility to simultaneously affect a_μ and the B_s system observables with Δ contributions.

In absence of the a_μ constraint, the bounds on $Y_{\tau s}Y^*_{\tau b}$ are significantly relaxed and are dominated by Δm_s and $\Delta m_s/\Delta m_d$ (see figure 6). $|Y_{\tau s}Y^*_{\tau b}|$ values of order 0.1 are allowed,

JHEP11(2011)002

however at the expense of fine-tuning the phase $\mathrm{Arg}(Y_{\tau s}Y^*_{\tau b})$ in order to obtain the right destructive interference with the SM contributions to the $B_{s,d}$ mass differences.

5 GUT implications

5.1 Framework

The color triplet leptoquark $(\overline{\mathbf{3}},\mathbf{1},4/3)$ emerges naturally in a theoretically well-motivated class of grand unified models. We will first demonstrate this in a framework of the SU(5) gauge group — the simplest group to encompass the SM gauge symmetry — and then proceed to discuss how and where it appears in the SO(10) setup.

5.1.1 SU(5) setup

The matter of the SM is assigned to the 10- and 5-dimensional SU(5) representations, i.e., $\mathbf{10}_i = (\mathbf{1},\mathbf{1},1)\oplus(\overline{\mathbf{3}},\mathbf{1},-2/3)\oplus(\mathbf{3},\mathbf{2},1/6)$ and $\bar{\mathbf{5}}_i = (\mathbf{1},\mathbf{2},-1/2)\oplus(\overline{\mathbf{3}},\mathbf{1},1/3)$, where $i(=1,2,3)$ denotes generation index [69]. This assignment dictates that the charged fermion masses and the entries of the CKM matrix originate, at the tree-level, through the couplings of the matter fields to the 5- and 45-dimensional Higgs representations only [70]. It has actually been shown that the phenomenological considerations require presence of both [71–76]. It turns out that the color triplet leptoquark is a part of the 45-dimensional representation. Namely, the relevant SM decomposition reads $\mathbf{45}\equiv(\Delta_1,\Delta_2,\Delta_3,\Delta_4,\Delta_5,\Delta_6,\Delta_7) = (\mathbf{8},\mathbf{2},1/2)\oplus(\overline{\mathbf{6}},\mathbf{1},-1/3)\oplus(\mathbf{3},\mathbf{3},-1/3)\oplus(\overline{\mathbf{3}},\mathbf{2},-7/6)\oplus(\mathbf{3},\mathbf{1},-1/3)\oplus(\overline{\mathbf{3}},\mathbf{1},4/3)\oplus(\mathbf{1},\mathbf{2},1/2)$. The color triplet thus appears in any SU(5) framework that relies purely on the scalar representations for the charged fermion mass generation.

Relevant contractions of the 45- and 5-dimensional Higgs representations, i.e., $\mathbf{45}$ and $\mathbf{5}$, with the matter fields, are $(Y_1)_{ij}\mathbf{10}_i\bar{\mathbf{5}}_j\mathbf{45}^*$, $(Y_2)_{ij}\mathbf{10}_i\mathbf{10}_j\mathbf{45}$, $(Y_3)_{ij}\mathbf{10}_i\bar{\mathbf{5}}_j\mathbf{5}^*$ and $(Y_4)_{ij}\mathbf{10}_i\mathbf{10}_j\mathbf{5}$, where Y_a, $a=1,2,3,4$, represent arbitrary Yukawa coupling matrices in flavor space. The charged fermion mass matrices at the unification scale accordingly read

$$M_D = -Y_1 v^*_{45} - \frac{1}{2}Y_3 v^*_5, \tag{5.1}$$

$$M_E = 3Y_1^T v^*_{45} - \frac{1}{2}Y_3^T v^*_5, \tag{5.2}$$

$$M_U = 2\sqrt{2}(Y_2 - Y_2^T)v_{45} - \sqrt{2}(Y_4 + Y_4^T)v_5, \tag{5.3}$$

where $\langle\mathbf{5}^5\rangle = v_5/\sqrt{2}$ and $\langle\mathbf{45}^{15}_1\rangle = \langle\mathbf{45}^{25}_2\rangle = \langle\mathbf{45}^{35}_3\rangle = v_{45}/\sqrt{2}$ represent appropriate vacuum expectation values. Note that $\mathbf{5}\equiv\mathbf{5}^\alpha$, $\mathbf{45}\equiv\mathbf{45}^{\alpha\beta}_\gamma$ and $|v_5|^2/2 + 12|v_{45}|^2 = v^2$, where $\alpha,\beta,\gamma = 1,\ldots,5$ represent SU(5) indices and $v(=246\,\mathrm{GeV})$ stands for the electroweak vacuum expectation value (VEV). (The VEV result has been introduced for the first time in ref. [6] and corrects the normalization presented in refs. [75, 77].) In SU(5) there could be an additional contribution to v from an SU(2) triplet scalar [78] but that contribution is supposed to be suppressed by a large symmetry breaking scale [79] and we accordingly neglect it. We also assume that both v_5 and v_{45} are real for simplicity.

In order to have consistent notation we identify Δ_6 with Δ in what follows. The lepton and baryon number violating Yukawa couplings of the triplet Δ to matter in the

JHEP11(2011)002

fermion mass eigenstate basis in the SU(5) framework are already given in eq. (2.2) if one makes the following identifications: $Y \equiv E_R^\dagger Y_1 D_R^*$ and $g \equiv 2\sqrt{2} U_R^\dagger [Y_2 - Y_2^T] U_R^*$. Here, E_R, D_R and U_R represent appropriate unitary transformations of the right-handed charged leptons, down-quarks and up-quarks. Our phenomenological study primarily relates to Yukawa couplings of Δ to the down-quark and charged lepton sectors. Clearly, these low-energy constraints on the leptoquark couplings to the matter could allow us to place constraints on the very Yukawa couplings and associated unitary transformations that show up in the charged fermion mass relations. These, on the other hand, might be pivotal in addressing the issue of matter stability [80].

Note that the antisymmetric nature of the color triplet couplings to the up-quark sector in eq. (2.2) is dictated by the group theory and is not affected by any change of basis. In other words, any unitary redefinition of fermion fields would preserve this property. We insist on this point for the following two reasons. Firstly, this is important since it is this unique feature of the Δ couplings to the up-quark sector that is responsible for an absence of the leading contributions towards proton decay due to Δ exchange [77]. Secondly, if, for some reason, Y_2 is a symmetric matrix, there would not be any coupling between Δ and the up sector. In other words, all g_{ij} elements in eq. (2.2) would be zero. If that was the case, Δ would not mediate proton decay. In fact that can happen, for example, if the scalar leptoquark Δ originates from an SO(10) setup as we discuss next.

5.1.2 SO(10) setup

Recall, one generation of the SM matter in the SO(10) framework is embedded in a single 16-dimensional representation. The allowed contractions of the matter fields to the Higgs sector, at the tree-level, are $(Y_{10})_{ij}\mathbf{16}_i\mathbf{16}_j\mathbf{10}$, $(Y_{120})_{ij}\mathbf{16}_i\mathbf{16}_j\mathbf{120}$ and $(Y_{126})_{ij}\mathbf{16}_i\mathbf{16}_j\overline{\mathbf{126}}$, where $\mathbf{10}$, $\mathbf{120}$ and $\overline{\mathbf{126}}$ are the scalar representations that all contain states with the quantum numbers of the SM doublet [70]. Here, $Y_{10}(= Y_{10}^T)$, $Y_{120}(= -Y_{120}^T)$ and $Y_{126}(= Y_{126}^T)$ represent complex Yukawa coupling matrices. As it turns out, the 45-dimensional representation of SU(5) is found in both the 120- and 126-dimensional representations [70]. The former one couples antisymmetrically to matter, thus preserving the absence of the leading contributions towards proton decay due to Δ exchange [77]. The latter one, on the other hand, couples symmetrically to matter. So, if Δ originates from the 126-dimensional representation of SO(10), it will not couple to the up-quark sector at all. Consequently, there will be no proton decay signatures related to Δ exchange in that case. Again, these properties are dictated by gauge symmetry and are preserved regardless of any redefinitions of the charged fermion fields. (Note that our findings on the absence of the up-quark sector couplings do not agree with the conclusions put forth in ref. [9] for the SO(10) case and in ref. [81] for the SU(5) case.)

The relevant mass matrices for the down-quarks and charged leptons in the SO(10) framework are

$$M_D = -Y_{126} v_{126}^* - \frac{1}{2} Y_{10} v_{10}^* + Y_{120}(v_{120}'^* + v_{120}''^*), \tag{5.4}$$

$$M_E = 3Y_{126} v_{126}^* - \frac{1}{2} Y_{10}^T v_{10}^* + Y_{120}(v_{120}'^* - 3v_{120}''^*), \tag{5.5}$$

JHEP11(2011)002

where v_{10}, v_{126}, v'_{120} and v''_{120} represent VEVs of the doublet components of the appropriate scalar representations. We will assume that the VEVs are real when needed for simplicity. (See ref. [82] for exact normalization with respect to the SM VEV.) Clearly, the observed mismatch between the charged lepton and down-quark masses requires a presence of either **120** or $\overline{\mathbf{126}}$, or both representations in the case without the **10**. The color triplet hence must appear in any SO(10) framework that relies purely on the scalar representations for the charged fermion mass generation.

We opt to start our analysis within a particular class of SU(5) models having in mind that the same procedure can be carried over into an SO(10) framework with appropriate modifications. In fact, towards the end of the next section we also address the SO(10) setup viability in view of its compatibility with phenomenological constraints on the couplings of the light colored scalar to the matter fields.

5.2 Numerical analysis

Our goal is to consistently implement all available constraints on the color triplet couplings to the down-quarks and charged leptons in order to study implications for the charged fermion Yukawa sector within a particular class of grand unified models. These models rely solely on the scalar representations in order to generate charged fermion masses.

We first single out a simple SU(5) setup with the 5-, 24- and 45-dimensional representations in the Higgs sector [71–76] and one 24-dimensional fermionic representation [76] to generate neutrino masses via combination of type I [83–87] and type III [88, 89] seesaw mechanisms for definiteness. We resort to this model since it has been explicitly demonstrated that it predicts proton decay signatures that are very close to the present experimental limits on the partial proton decay lifetimes for the mass of Δ in the range accessible in collider experiments [2]. (The model is a renormalizable version of the scenario first proposed in [90] and further analyzed in [91, 92].) Moreover, it shares the same mass relations given in eqs. (5.1), (5.2) and (5.3) with all other SU(5) scenarios that rely on the use of the 5- and 45-dimensional scalar representations.

We start with the following relations that are valid at the unification scale

$$E_R^\dagger D_L M_D^{\rm diag} = \left(-\frac{1}{2} E_R^\dagger Y_3 D_R^* v_5 - Y v_{45} \right), \tag{5.6}$$

$$M_E^{\rm diag} E_L^T D_R^* = \left(-\frac{1}{2} E_R^\dagger Y_3 D_R^* v_5 + 3 Y v_{45} \right), \tag{5.7}$$

where $M_D^{\rm diag}$ and $M_E^{\rm diag}$ are diagonal mass matrices for down quarks and charged leptons, respectively. Our convention is such that $M_D = D_L M_D^{\rm diag} D_R^T$ and $M_E = E_L M_E^{\rm diag} E_R^T$, where D_L and E_L represent appropriate unitary transformations of the left-handed down quarks and charged leptons. Note that our phenomenological considerations yield constrains on the form of Y that are valid at low energies only. It is thus essential to propagate constraints on $(Y)_{ij}$, $i,j = 1,2,3$, as well as the entries of $M_D^{\rm diag}$ and $M_E^{\rm diag}$ to the GUT scale to extract accurate information on v_{45} and unitary matrices $E_R^\dagger D_L$ and $E_L^T D_R^*$.

JHEP11(2011)002

running mass at M_Z	running mass at $M_{\rm GUT}$
$m_b(M_Z) = 2.89 \pm 0.11\,\text{GeV}$	$m_b(M_{\rm GUT}) = 0.782\,\text{GeV}$
$m_s(M_Z) = 56 \pm 16\,\text{MeV}$	$m_s(M_{\rm GUT}) = 19\,\text{MeV}$
$m_d(M_Z) = 3.0 \pm 1.2\,\text{MeV}$	$m_d(M_{\rm GUT}) = 1.1\,\text{MeV}$
$m_\tau(M_Z) = 1746.45^{+0.29}_{-0.26}\,\text{MeV}$	$m_\tau(M_{\rm GUT}) = 1561.4\,\text{MeV}$
$m_\mu(M_Z) = 102.72899(44)\,\text{MeV}$	$m_\mu(M_{\rm GUT}) = 91.84\,\text{MeV}$
$m_e(M_Z) = 0.4866613(36)\,\text{MeV}$	$m_e(M_{\rm GUT}) = 0.4350\,\text{MeV}$

Table 8. Input parameters for the relevant fermion masses at the M_Z scale and the corresponding values at the GUT scale ($M_{\rm GUT} = 10^{16}\,\text{GeV}$) in a non-supersymmetric framework.

Again, the phenomenological bounds we derive constrain the matrix Y appearing on the right-hand side of a relation

$$E_R^\dagger D_L M_D^{\rm diag} - M_E^{\rm diag} E_L^T D_R^* = -4 Y v_{45}. \tag{5.8}$$

What is not known are the overall scale of the right-hand side set by v_{45} and the unitary transformations given by $E_R^\dagger D_L$ and $E_L^T D_R^*$. In order to perform numerical analysis and implement inferred bounds we first parametrize $E_R^\dagger D_L$ and $E_L^T D_R^*$ using a generic form

$$U = \begin{pmatrix} e^{i\alpha_1} & 0 & 0 \\ 0 & e^{i\alpha_2} & 0 \\ 0 & 0 & e^{i\alpha_3} \end{pmatrix} \begin{pmatrix} c_{12}c_{13} & s_{12}c_{13} & s_{13}e^{-i\alpha_4} \\ -s_{12}c_{23} - c_{12}s_{23}s_{13}e^{i\alpha_4} & c_{12}c_{23} - s_{12}s_{23}s_{13}e^{i\alpha_4} & s_{23}c_{13} \\ s_{12}s_{23} - c_{12}c_{23}s_{13}e^{i\alpha_4} & -c_{12}s_{23} - s_{12}c_{23}s_{13}e^{i\alpha_4} & c_{23}c_{13} \end{pmatrix} \begin{pmatrix} e^{i\alpha_5} & 0 & 0 \\ 0 & e^{i\alpha_6} & 0 \\ 0 & 0 & 1 \end{pmatrix}, \tag{5.9}$$

where $s_{ab} \equiv \sin\theta_{ab}$, $c_{ab} \equiv \cos\theta_{ab}$, and α_i, $i = 1, \ldots, 6$, are phases. We then randomly generate the total of nineteen parameters and check whether the left-hand side of eq. (5.8) satisfies all phenomenological constraints. (We also vary the four parameters of the CKM matrix as well as η_1, η_2 and η_3 — QCD parameters entering $K - \bar{K}$ mixing — in order to have consistent constraints on the Y entries as described in section 3.) This process is repeated until the available parameter space is thought to be exhausted. The down-quark and charged lepton masses at the GUT scale are considered as input and the relevant values we generate and use within this particular framework are given in table 8. The GUT scale is taken to be $M_{\rm GUT} = 10^{16}\,\text{GeV}$ and we only propagate and use the central values for the down-quark and charged lepton masses.

Note that the need to accommodate experimental results on a_μ basically sets the scale for the Y entries. To be precise, it requires that $\sum_{i=1,2,3} |Y_{2i}|^2$ satisfies eq. (3.52). This in turn should fix the value or range of allowed values of v_{45} since the scale of the left-hand side of eq. (5.8) is set by the known fermion masses. One can then use this information to determine v_5 via $|v_5|^2/2 + 12|v_{45}|^2 = v^2$. To be conservative we not only vary $\sum_{i=1,2,3} |Y_{2i}|^2$ within the $1\,\sigma$ and $2\,\sigma$ ranges but accommodate for the effect of the RGE running of our constraints from the low scale to the grand unified scale. We take that effect to be within the bounds set by the following scaling factors: 1.1–3.7. These scaling factors correspond to the maximal changes in the charged lepton and down quark masses as they are propagated

JHEP11(2011)002

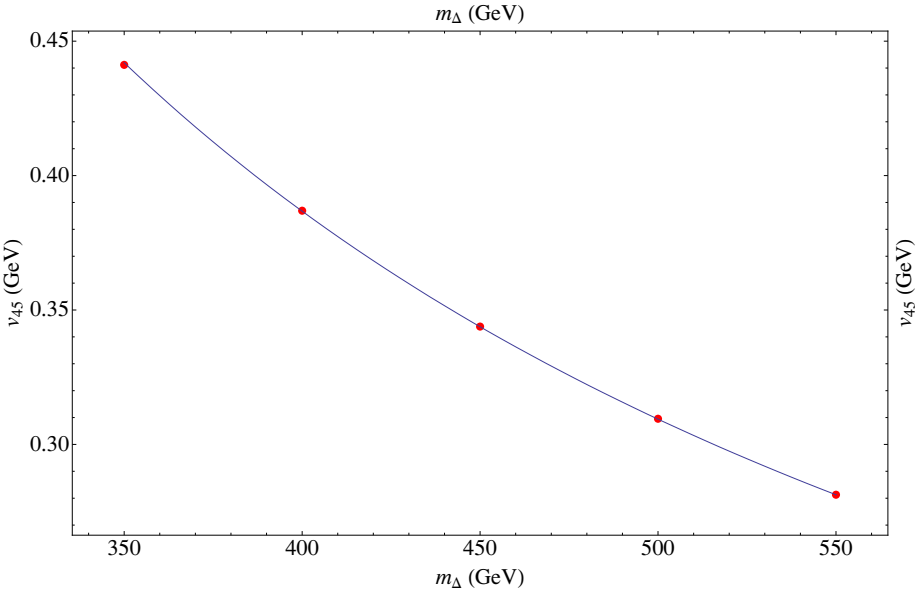

Figure 7. Upper bound on v_{45} as a function of m_Δ. Data are generated for a discrete set of m_Δ values that are shown as dots. The curve is an interpolation that carries an m_Δ^{-1} dependence.

from low scale to the GUT scale. Again, we take the GUT scale to be $M_{\rm GUT} = 10^{16}$ GeV for simplicity. (The exact dependence of the GUT scale on the scalar particle mass spectrum within this particular SU(5) model is known and has been worked out in detail in ref. [2]. The change in the GUT scale or, correspondingly, the scalar particle mass spectrum also affects propagation of fermion masses but that effect is rather small for the scenario when Δ is light as the GUT scale is then limited within a very narrow range [2].)

The upper limit on v_{45} which we obtain by randomly choosing the entries of $E_R^\dagger D_L$ and $E_L^T D_R^*$ is shown in figure 7. Clearly, the bound should drop as m_Δ grows since v_{45} needs to compensate the growth of the appropriate values of Y that satisfy the a_μ constraint of eq. (3.52). For practical purposes, we generate this conservative limit when only eq. (3.52) is satisfied for a finite set of fixed values of m_Δ. These correspond to dots in figure 7. In our numerical study we limit the m_Δ range due to the existence of both the lower and upper bounds on its value. The lower experimental bound on m_Δ comes from direct experimental searches. The most stringent one originates from dedicated searches for pair production of leptoquarks in pp collisions at LHC and it reads $m_\Delta > 384\,\text{GeV}$ [93] ($m_\Delta > 422\,\text{GeV}$ [94]) for the so-called first-generation (second-generation) leptoquarks assuming these decay exclusively to an electron (muon) and a hadronic jet. While these bounds are not necessarily applicable to our framework, since Δ can also decay to a top quark and a hadronic jet, we have verified that the corresponding branching ratio is always below 30% in the region of parameter space where Δ resolves both the $t\bar{t}$ FBA and the a_μ puzzles. The upper bound on m_Δ, on the other hand, originates from perturbativity constraints on entries of Y that should not exceed $\sqrt{4\pi}$. We find that bound to be $m_\Delta \lesssim 560\,\text{GeV}$.

After an extensive numerical study we fail to generate a single satisfactory solution to all the constraints using eq. (5.8) as a starting point. We trace the difficulty of finding a

JHEP11(2011)002

viable numerical solution to the facts that (i) the down-quark and charged lepton sectors do not exhibit a strong mass hierarchy that is present in the up-quark sector and (ii) the misalignment between the masses of the down-quarks and charged leptons that belong to the same generation is sufficiently large to prevent necessary cancellations. For example, a generic form of the left-hand side in eq. (5.8) can be represented as follows

$$\begin{pmatrix} 0 & 0 & 0 \\ 0 & 0 & 0 \\ \blacksquare & \blacksquare & \blacksquare \end{pmatrix} + \begin{pmatrix} 0 & 0 & \bullet \\ 0 & 0 & \bullet \\ 0 & 0 & \bullet \end{pmatrix} . \tag{5.10}$$

Here ■ (•) stands for an order m_τ (m_b) element. Clearly, the only potentially viable scenario for this form to describe matrix Y, pictorially given in eq. (4.5), would be the one where the 23 element dominates. The 31 and 32 elements should accordingly be suppressed by effectively setting the angles θ_{13} and θ_{23} from $E_L^T D_R^*$ to zero. This, however, leaves the 33 element on the left-hand side of eq. (5.8) to be proportional to $m_\tau - m_b(E_R^\dagger D_L)_{33}$. As $m_\tau(M_{\rm GUT}) \sim 2m_b(M_{\rm GUT})$ in the scenario at hand and $|(E_R^\dagger D_L)_{33}| \leq 1$, the absolute value of the 33 element turns out to always be greater than the absolute value of the 23 element, in contrast to what is needed. One could try to see if there is a possibility to have a satisfactory numerical solution within the supersymmetric framework where, for example, the mismatch between b and τ varies a lot with the change in the $\tan\beta$ parameter. This scenario, although it does help in suppressing the 33 element, also fails due to the difficulty to accommodate small enough elements in the 1-2 block of the left-hand side of eq. (5.8). Namely, once the freedom to set the 13 and 33 elements to be small by tuning the angles in $E_R^\dagger D_L$ is used there is not enough parameters left over to tune the 1-2 block to the desired form. For example, since $m_e(M_{\rm GUT})/m_b(M_{\rm GUT}) \sim m_d(M_{\rm GUT})/m_b(M_{\rm GUT}) \sim 10^{-4}$, the 11 element is always bigger than the required limit of 10^{-6}. In short, the SU(5) scenarios with a light triplet scalar that rely on the use of the 5- and 45-dimensional scalar representations to generate charged fermion masses at the tree level fail to accommodate the Yukawa structure needed to explain the a_μ puzzle while satisfying all other phenomenological constraints.

Let us now discuss implications of our findings with respect to their compatibility with the most commonly encountered SO(10) scenarios. Recall, the only representations of SO(10) that could, at the tree-level, yield contributions to the charged fermion masses are the **10**, **120** and $\overline{\mathbf{126}}$. And, as we have pointed out in section 5.1, Δ can originate from either 120- or 126-dimensional representation of SO(10).

If Δ is part of the 126-dimensional Higgs it would not couple to the up-quark sector since the relevant couplings to matter are symmetric whereas Δ needs to couple in an anti-symmetric manner to the up-quarks. If, in addition to the $\overline{\mathbf{126}}$, one uses a 10-dimensional scalar representation to generate the charged fermion masses the corresponding mass matrices will all be symmetric. This, on the other hand, changes the transformations that generate mass eigenstate basis from bi-unitary into congruent form. This significantly reduces the number of free parameters yielding the following mass relation

$$U M_D^{\rm diag} - M_E^{\rm diag} U^* = -4 Y v_{126}, \tag{5.11}$$

JHEP11(2011)002

where $U = E_R^\dagger D_R$, $E_R = E_L$ and $D_R = D_L$. This relation also corresponds to the SU(5) scenario when all Yukawa matrices in the down-quark and charged lepton sectors are symmetric. Obviously, this case is much more restrictive since we have only one unitary matrix U to vary. It is thus clear that this scenario cannot be viable if we implement all the constraints on the form of Y. Hence, the case when Yukawa couplings in the charged lepton and down-quark sectors are symmetric, including the case with the 10- and 126-dimensional scalar representations in SO(10), is not compatible with possibility to have light Δ as an explanation for observed anomalies.

The scenario with the 10- and 120-dimensional representations in the Higgs sector is also not realistic. In fact, that scenario resembles the SU(5) scenario that proved to be inadequate to accommodate the form of Y matrix. Moreover, the 10- and 120-dimensional representation scenario cannot explain observed fermion masses as was demonstrated in the low-scale supersymmetric case [95]. In fact, even the $\overline{\mathbf{126}}$ and $\mathbf{10}$ of Higgs scenario would require complex $\mathbf{10}$ just to meet the charged fermion mass constraints [82] in the non-supersymmetric case. This finally leaves, as the only viable possibility, the most general scenario with the 10-, 120- and 126-dimensional representations as the one that could accommodate constraints generated by the Δ phenomenology in the SO(10) framework. The relevant relation, in that scenario, reads

$$E_R^\dagger D_L M_D^{\rm diag} - M_E^{\rm diag} E_L^T D_R^* = -4 E_R^\dagger Y_{126} D_R^* v_{126} + 4 E_R^\dagger Y_{120} D_R^* v''_{120}. \tag{5.12}$$

Clearly, $E_R^\dagger Y_{126} D_R^*$ ($E_R^\dagger Y_{120} D_R^*$) would be proportional to Y for Δ originating from $\overline{\mathbf{126}}$ ($\mathbf{120}$). In both cases there are more than enough parameters to accommodate required form of Y. Note, however, that our conservative estimate for the upper bound on v_{45} as shown in figure 7 should still be applicable on either v_{126} or v''_{120}. For example, if we identify $E_R^\dagger Y_{126} D_R^*$ ($E_R^\dagger Y_{120} D_R^*$) with Y it is clear that the left-hand side of eq. (5.12) cannot be dominated by the term proportional to v''_{120} (v_{126}). If the opposite was true, we would obtain $E_R^\dagger Y_{126} D_R^* \sim E_R^\dagger Y_{120} D_R^*$ which certainly cannot hold as Y_{126} is symmetric and Y_{120} is antisymmetric. To conclude, the only viable candidate that can accommodate Y is the SO(10) scenario with the $\mathbf{10}$, $\mathbf{120}$ and $\overline{\mathbf{126}}$.

6 Conclusions

We have investigated the role of a colored weak singlet scalar possibly addressing the $t\bar{t}$ FBA puzzle in flavor changing processes and precision observables of down-quarks and charged leptons. The magnitude of the predicted effects is governed by the mass of the scalar (which we normalize to 400 GeV as preferred by the $t\bar{t}$ phenomenology), and (generic) complex matrix Y acting in quark and lepton flavor-space. Y is the central object of this analysis.

Virtual contributions of the considered scalar affect many observables and in order to obtain insight into the Y structure we have analyzed a plethora of rare quark and lepton processes, some of them well measured, others bounded from above. In particular we have considered FCNC and CP violating observables in K and $B_{d,s}$ meson systems, (lepton flavor violating) dileptonic decays of neutral mesons, $\mu - e$ conversion in nuclei, anomalous magnetic moments of charged leptons, and lepton flavor violating decays of the muon and

JHEP11(2011)002

τ lepton. For completeness, we have also considered effects in the $Z \to b\bar{b}$ decay width. We have properly accounted for SM contributions to the relevant observables where needed.

Then we have performed a global χ^2 fit of the Y matrix elements and found an excellent agreement with all the considered constraints. We have confirmed that the couplings to electrons are strongly suppressed. The most salient finding is the explanation of the anomalous magnetic moment of muon, which requires the muon coupling to a single generation down-quark to be of order one. Combined with LFV B and τ decay constraints, this leads to strong limits on the tau lepton couplings to down quarks which in turn exclude the possibility [52] to simultaneously explain the measured large CP-violating mixing phase in the B_s sector or a large enhancement of absorptive mixing amplitude Γ_{12s} in this model. Even in absence of the a_μ constraint, the $B_s - \bar{B}_s$ mass difference measurements alone constrain the relevant leptoquark couplings and a large new absorptive contribution in $B_s - \bar{B}_s$ mixing cannot be generated. Using a value of $|V_{ub}|$ preferred by the measured branching fraction of $B \to \tau\nu$ we find that this model can modify the $B_d - \bar{B}_d$ mixing amplitude sufficiently to remove the tension between the two observables. However, in this case the anomalous magnetic moment of the muon cannot be explained.

We have systematically implemented all the phenomenological constraints in a class of SU(5) models where all the fermion masses are generated at the tree-level to find out that the explanation of the a_μ anomaly requires the vacuum expectation value of the 45-dimensional representation to be of the order of 10^{-1} GeV. This result implies that the up-quark couplings, in this setup, are symmetric in nature. This in turn makes predictions for certain partial proton decay lifetimes very accurate. We have also shown that the symmetric scenario for the Yukawa couplings in the down-quark and charged lepton case is not compatible with the constraints due to the presence of light Δ and discussed implications for the SO(10) type of unification. The simplest of possible realizations of both SO(10) and SU(5) with the symmetric Yukawa sector, that could accommodate observed fermion masses, are shown not to be viable unless Δ is heavy enough not to play any role in low-energy phenomenology.

We conclude by noting, that the couplings of the leptoquark in question to the matter fields, in the physical basis, are always dominated by just one of the entries of the second row of matrix Y. That entry is at least two orders of magnitude larger than any other entry. This property puts this particular leptoquark effectively in the so-called second generation category. Moreover, as it does not couple to neutrinos, the bound extracted from the recent LHC data for the second-generation leptoquarks [94] is truly applicable in this case and reads $m_\Delta \gtrsim 380\,\text{GeV}$, accounting for the reduced $\Delta \to \mu j$ branching ratio of order $\mathcal{B} \gtrsim 0.7$ due to the presence of the $\Delta \to tj$ decay channel [2]. This and the upper bound on its mass — $m_\Delta < 560\,\text{GeV}$ — that originates from simple perturbativity arguments thus place it in a very narrow window of discovery.

Acknowledgments

We thank Ulrich Haisch for pointing out several important B decay modes missing in the first version of the analysis and for useful discussions regarding the B_s mixing phenomenol-

JHEP11(2011)002

ogy. We also acknowledge useful discussions with Jure Zupan. N.K. thanks François Le Diberder for invaluable advice on the fit part. I.D. thanks the Institut "Jožef Stefan" where part of this work was completed for their hospitality. This work is supported in part by the Slovenian Research Agency.

A One loop contributions of Δ to R_b

We are working in the massless limit $m_\ell = m_b = 0$ and in $d = 4+\epsilon$ dimensions to regularize UV divergence. The first two diagrams in figure 3 give the following contribution to the 1-particle irreducible (1PI) amplitude

$$\mathcal{A}^{\Delta,1\mathrm{PI}} = \mathrm{i} g_Z \sin^2\theta_W \frac{\sum_\ell |Y_{\ell b}|^2}{(4\pi)^2} C_\epsilon \Bigg[-\frac{1}{3\epsilon} + \frac{1}{6x_Z^2}\Big[9x_Z^2 - 2x_Z + \log(x_Z)\big(3x_Z^2 - 6x_Z + 6\log(1+x_Z)\big) \tag{A.1}$$
$$-8f_1 + 4f_2(2x_Z - x_Z^2) + 6\mathrm{Li}_2(-x_Z)) - \mathrm{i}\pi\Big(3x_Z^2 - 6x_Z + 6\log(1+x_Z)\Big)\Big]\Bigg] \mathcal{A}_R \,,$$

where $C_\epsilon = m_\Delta^\epsilon/(4\pi)^{\epsilon/2}\Gamma(1-\epsilon/2)$ and f_1, f_2 are auxiliary functions defined as

$$f_1 = 4\arctan\left(\sqrt{\frac{x_Z}{4-x_Z}}\right)\arctan\left(\frac{\sqrt{x_Z(4-x_Z)}}{2-x_Z}\right) + \mathrm{Li}_2(x_Z) \tag{A.2}$$
$$+2\mathrm{Re}\left\{\mathrm{Li}_2\left(\frac{x_Z}{2} + \frac{\mathrm{i}}{2}\sqrt{x_Z(4-x_Z)}\right) - \mathrm{Li}_2\left(\frac{x_Z}{2}(3-x_Z) - \frac{\mathrm{i}}{2}(1-x_Z)\sqrt{x_Z(4-x_Z)}\right)\right\},$$
$$f_2 = 2\sqrt{\frac{4-x_Z}{x_Z}}\arctan\left(\sqrt{\frac{x_Z}{4-x_Z}}\right). \tag{A.3}$$

In addition to graphs in figure 3 there are one loop contributions of Δ to b-quark self-energy, corresponding to on-shell field renormalization of the b-quark field

$$Z_b = 1 + \delta_b \,, \qquad \delta_b = -\frac{1}{2}\frac{\sum_\ell |Y_{\ell b}|^2}{(4\pi)^2} C_\epsilon \left[-\frac{2}{\epsilon} + \frac{1}{2}\right]. \tag{A.4}$$

Combining the tree-level SM with 1PI diagrams of Δ and the field strength renormalization we obtain the UV-finite amplitude

$$\mathcal{A} = Z_b(\mathcal{A}^{\mathrm{tree}} + \mathcal{A}^{\Delta,1\mathrm{PI}}) = \mathrm{i} g_Z \Big[(g_R^0 + \delta g_R)\mathcal{A}_R + g_L^0 \mathcal{A}_L\Big] \,, \tag{A.5}$$

where the change of right-handed coupling, δg_R, is given in eq. (3.59).

References

[1] J.F. Kamenik, J. Shu and J. Zupan, *Review of new physics effects in $t\bar{t}$ production*, arXiv:1107.5257 [INSPIRE].

JHEP11(2011)002

[2] I. Doršner, S. Fajfer, J.F. Kamenik and N. Košnik, *Light colored scalars from grand unification and the forward-backward asymmetry in $t\bar{t}$ production*, *Phys. Rev.* **D 81** (2010) 055009 [arXiv:0912.0972] [INSPIRE].

[3] M.I. Gresham, I.-W. Kim and K.M. Zurek, *On models of new physics for the Tevatron top A_{FB}*, *Phys. Rev.* **D 83** (2011) 114027 [arXiv:1103.3501] [INSPIRE].

[4] K. Blum, Y. Hochberg and Y. Nir, *Scalar-mediated $t\bar{t}$ forward-backward asymmetry*, arXiv:1107.4350 [INSPIRE].

[5] M.I. Gresham, I.-W. Kim and K.M. Zurek, *Tevatron top A_{FB} versus LHC top physics*, arXiv:1107.4364 [INSPIRE].

[6] I. Doršner, S. Fajfer, J.F. Kamenik and N. Košnik, *Light colored scalar as messenger of up-quark flavor dynamics in grand unified theories*, *Phys. Rev.* **D 82** (2010) 094015 [arXiv:1007.2604] [INSPIRE].

[7] H. Georgi, *Unified gauge theories*, in the *Proceedings of Theories and Experiments in High-Energy Physics*, Center for Theoretical Physics, University of Miami, Miami U.S.A. (1975) [INSPIRE].

[8] H. Fritzsch and P. Minkowski, *Unified interactions of leptons and hadrons*, *Annals Phys.* **93** (1975) 193 [INSPIRE].

[9] K.M. Patel and P. Sharma, *Forward-backward asymmetry in top quark production from light colored scalars in* SO(10) *model*, *JHEP* **04** (2011) 085 [arXiv:1102.4736] [INSPIRE].

[10] MUON G-2 collaboration, G. Bennett et al., *Measurement of the negative muon anomalous magnetic moment to* 0.7 *ppm*, *Phys. Rev. Lett.* **92** (2004) 161802 [hep-ex/0401008] [INSPIRE].

[11] F. Jegerlehner, *Essentials of the muon g-2*, *Acta Phys. Polon.* **B 38** (2007) 3021 [hep-ph/0703125] [INSPIRE].

[12] CDF collaboration, T. Aaltonen et al., *First flavor-tagged determination of bounds on mixing-induced CP-violation in $B_s^0 \to J/\psi\phi$ decays*, *Phys. Rev. Lett.* **100** (2008) 161802 [arXiv:0712.2397] [INSPIRE].

[13] DØ collaboration, V. Abazov et al., *Measurement of B_s^0 mixing parameters from the flavor-tagged decay $B_s^0 \to J/\psi\phi$*, *Phys. Rev. Lett.* **101** (2008) 241801 [arXiv:0802.2255] [INSPIRE].

[14] DØ collaboration, *Updated combined DØ results on $\Delta\Gamma_s$ versus CP-violating phase $\phi_s^{J/\psi\phi}$*, note 6093-CONF, Fermilab, Batavia U.S.A. (2010).

[15] CDF collaboration, *An updated measurement of the CP violating phase $\beta_s^{J/\psi\phi}$ in $B_s^0 \to J/\psi\phi$ decays using* 5.2 fb^{-1} *of integrated luminosity*, public note 10206, Fermilab, Batavia U.S.A. (2010).

[16] DØ collaboration, V.M. Abazov et al., *Evidence for an anomalous like-sign dimuon charge asymmetry*, *Phys. Rev.* **D 82** (2010) 032001 [arXiv:1005.2757] [INSPIRE].

[17] DØ collaboration, V.M. Abazov et al., *Measurement of the anomalous like-sign dimuon charge asymmetry with* 9 fb^{-1} *of $p\bar{p}$ collisions*, *Phys. Rev.* **D 84** (2011) 052007 [arXiv:1106.6308] [INSPIRE].

[18] Z. Ligeti, M. Papucci, G. Perez and J. Zupan, *Implications of the dimuon CP asymmetry in $B_{d,s}$ decays*, *Phys. Rev. Lett.* **105** (2010) 131601 [arXiv:1006.0432] [INSPIRE].

[19] A. Lenz, U. Nierste, J. Charles, S. Descotes-Genon, A. Jantsch, et al., *Anatomy of new physics in B-$\bar{B}$ mixing*, *Phys. Rev.* **D 83** (2011) 036004 [arXiv:1008.1593] [INSPIRE].

JHEP11(2011)002

[20] Y. Grossman, *The B_s width difference beyond the standard model*, *Phys. Lett.* **B 380** (1996) 99 [hep-ph/9603244] [INSPIRE].

[21] J.P. Saha, B. Misra and A. Kundu, *Constraining scalar leptoquarks from the K and B sectors*, *Phys. Rev.* **D 81** (2010) 095011 [arXiv:1003.1384] [INSPIRE].

[22] L.J. Hall, K. Jedamzik, J. March-Russell and S.M. West, *Freeze-in production of FIMP dark matter*, *JHEP* **03** (2010) 080 [arXiv:0911.1120] [INSPIRE].

[23] Particle Data Group collaboration, K. Nakamura et al., *Review of particle physics*, *J. Phys. G* **G 37** (2010) 075021 [INSPIRE].

[24] CDF and DØ collaboration, *Combination of CDF and DØ results on the mass of the top quark using up to* 5.6 fb^{-1} *of data*, arXiv:1007.3178 [INSPIRE].

[25] G. Isidori and R. Unterdorfer, *On the short distance constraints from $K_{L,S} \to \mu^+\mu^-$*, *JHEP* **01** (2004) 009 [hep-ph/0311084] [INSPIRE].

[26] G. D'Ambrosio, G. Isidori and J. Portoles, *Can we extract short distance information from $B(K_L \to \mu^+\mu^-)$?*, *Phys. Lett.* **B 423** (1998) 385 [hep-ph/9708326] [INSPIRE].

[27] J. Laiho, E. Lunghi and R.S. Van de Water, *Lattice QCD inputs to the CKM unitarity triangle analysis*, *Phys. Rev.* **D 81** (2010) 034503 [arXiv:0910.2928] [INSPIRE].

[28] G. Valencia, *Long distance contribution to $K_L \to \ell^+\ell^-$*, *Nucl. Phys.* **B 517** (1998) 339 [hep-ph/9711377] [INSPIRE].

[29] KLOE collaboration, F. Ambrosino et al., *Search for the $K_S \to e^+e^-$ decay with the KLOE detector*, *Phys. Lett.* **B 672** (2009) 203 [arXiv:0811.1007] [INSPIRE].

[30] G. Ecker and A. Pich, *The longitudinal muon polarization in $K_L \to \mu^+\mu^-$*, *Nucl. Phys.* **B 366** (1991) 189 [INSPIRE].

[31] LHCb collaboration, J. Serrano, *Search for the very rare decays $B_{s/d} \to \mu^+\mu^-$ at LHCb*, LHCb-TALK-2011-143, CERN, Geneva Switzerland (2011).

[32] BABAR collaboration, P.F. Harrison and H.R. Quinn eds., *The BABAR physics book: physics at an asymmetric B factory*, SLAC report SLAC-R-50 4, Stanford U.S.A. (1998).

[33] BABAR collaboration, B. Aubert et al., *A search for the rare decay $B^0 \to \tau^+\tau^-$ at BABAR*, *Phys. Rev. Lett.* **96** (2006) 241802 [hep-ex/0511015] [INSPIRE].

[34] S. Descotes-Genon, D. Ghosh, J. Matias and M. Ramon, *Exploring new physics in the C7-C7′ plane*, *JHEP* **06** (2011) 099 [arXiv:1104.3342] [INSPIRE].

[35] C. Bobeth, P. Gambino, M. Gorbahn and U. Haisch, *Complete NNLO QCD analysis of $\bar{B} \to X_s\ell^+\ell^-$ and higher order electroweak effects*, *JHEP* **04** (2004) 071 [hep-ph/0312090] [INSPIRE].

[36] BABAR collaboration, B. Aubert et al., *Measurement of the $B \to X_s\ell^+\ell^-$ branching fraction with a sum over exclusive modes*, *Phys. Rev. Lett.* **93** (2004) 081802 [hep-ex/0404006] [INSPIRE].

[37] Belle collaboration, M. Iwasaki et al., *Improved measurement of the electroweak penguin process $B \to X_s\ell^+\ell^-$*, *Phys. Rev.* **D 72** (2005) 092005 [hep-ex/0503044] [INSPIRE].

[38] T. Huber, T. Hurth and E. Lunghi, *Logarithmically enhanced corrections to the decay rate and forward backward asymmetry in $\bar{B} \to X_s\ell^+\ell^-$*, *Nucl. Phys.* **B 802** (2008) 40 [arXiv:0712.3009] [INSPIRE].

[39] P. Ball and R. Zwicky, *New results on $B \to \pi, K, \eta$ decay form factors from light-cone sum rules*, *Phys. Rev.* **D 71** (2005) 014015 [hep-ph/0406232] [INSPIRE].

JHEP11(2011)002

[40] A. Khodjamirian, T. Mannel, N. Offen and Y.-M. Wang, *$B \to \pi \ell \nu_l$ width and $|V_{ub}|$ from QCD light-cone sum rules*, *Phys. Rev.* **D 83** (2011) 094031 [arXiv:1103.2655] [INSPIRE].

[41] T. Feldmann, P. Kroll and B. Stech, *Mixing and decay constants of pseudoscalar mesons: the sequel*, *Phys. Lett.* **B 449** (1999) 339 [hep-ph/9812269] [INSPIRE].

[42] J.L. Rosner and S. Stone, *Leptonic decays of charged pseudoscalar mesons*, arXiv:1002.1655 [INSPIRE].

[43] R. Kitano, M. Koike and Y. Okada, *Detailed calculation of lepton flavor violating muon electron conversion rate for various nuclei*, *Phys. Rev.* **D 66** (2002) 096002 [hep-ph/0203110] [INSPIRE].

[44] SINDRUM II collaboration, C. Dohmen et al., *Test of lepton flavor conservation in $\mu \to e$ conversion on titanium*, *Phys. Lett.* **B 317** (1993) 631 [INSPIRE].

[45] SINDRUM II collaboration, W.H. Bertl et al., *A search for muon to electron conversion in muonic gold*, *Eur. Phys. J.* **C 47** (2006) 337 [INSPIRE].

[46] A.J. Buras, M. Jamin and P.H. Weisz, *Leading and next-to-leading QCD corrections to ϵ parameter and B^0-$\bar{B}^0$ mixing in the presence of a heavy top quark*, *Nucl. Phys.* **B 347** (1990) 491 [INSPIRE].

[47] T. Inami and C. Lim, *Effects of superheavy quarks and leptons in low-energy weak processes $k_L \to \mu \bar{n} u$, $K^+ \to \pi^+ \nu \bar{\nu}$ and $K^0 \leftrightarrow \bar{K}^0$*, *Prog. Theor. Phys.* **65** (1981) 297 [INSPIRE].

[48] A.J. Buras, D. Guadagnoli and G. Isidori, *On ϵ_K beyond lowest order in the operator product expansion*, *Phys. Lett.* **B 688** (2010) 309 [arXiv:1002.3612] [INSPIRE].

[49] S. Herrlich and U. Nierste, *Enhancement of the K_L-K_S mass difference by short distance QCD corrections beyond leading logarithms*, *Nucl. Phys.* **B 419** (1994) 292 [hep-ph/9310311] [INSPIRE].

[50] A.J. Buras, *Climbing NLO and NNLO summits of weak decays*, arXiv:1102.5650 [INSPIRE].

[51] J. Brod and M. Gorbahn, *ϵ_K at Next-to-Next-to-Leading Order: the charm-top-quark contribution*, *Phys. Rev.* **D 82** (2010) 094026 [arXiv:1007.0684] [INSPIRE].

[52] A. Dighe, A. Kundu and S. Nandi, *Enhanced B_s-$\bar{B}_s$ lifetime difference and anomalous like-sign dimuon charge asymmetry from new physics in $B_s \to \tau^+ \tau^-$*, *Phys. Rev.* **D 82** (2010) 031502 [arXiv:1005.4051] [INSPIRE].

[53] A.J. Buras, *Weak Hamiltonian, CP-violation and rare decays*, to appear in *Probing the Standard Model of Particle Interactions*, F. David and R. Gupta eds., Elsevier Science B.V., The Netherlands (1998) [hep-ph/9806471] [INSPIRE].

[54] Heavy Flavor Averaging Group collaboration, D. Asner et al., *Averages of b-hadron, c-hadron and τ-lepton properties*, arXiv:1010.1589 [INSPIRE].

[55] C.W. Bauer and N.D. Dunn, *Comment on new physics contributions to Γ_{12}^s*, *Phys. Lett.* **B 696** (2011) 362 [arXiv:1006.1629] [INSPIRE].

[56] J. Urban, F. Krauss, U. Jentschura and G. Soff, *Next-to-leading order QCD corrections for the B^0-$\bar{B}^0$ mixing with an extended Higgs sector*, *Nucl. Phys.* **B 523** (1998) 40 [hep-ph/9710245] [INSPIRE].

[57] F. Jegerlehner and A. Nyffeler, *The muon g-2*, *Phys. Rept.* **477** (2009) 1 [arXiv:0902.3360] [INSPIRE].

[58] D. Chakraverty, D. Choudhury and A. Datta, *A nonsupersymmetric resolution of the anomalous muon magnetic moment*, *Phys. Lett.* **B 506** (2001) 103 [hep-ph/0102180] [INSPIRE].

JHEP11(2011)002

[59] MEG collaboration, J. Adam et al., *New limit on the lepton-flavour violating decay* $\mu^+ \to e^+\gamma$, arXiv:1107.5547 [INSPIRE].

[60] R.J. Oakes, J.M. Yang and B.-L. Young, *Implications of LEP/SLD data for new physics in* $Zb\bar{b}$ *couplings*, *Phys. Rev.* **D 61** (2000) 075007 [hep-ph/9911388] [INSPIRE].

[61] MEG collaboration, S. Dussoni, *Searching for lepton flavor violation with the MEG experiment (or looking for flying pigs)*, *Nucl. Phys. Proc. Suppl.* **187** (2009) 109 [INSPIRE].

[62] MEG collaboration, J. Adam et al., *A limit for the* $\mu \to e\gamma$ *decay from the MEG experiment*, *Nucl. Phys.* **B 834** (2010) 1 [arXiv:0908.2594] [INSPIRE].

[63] SuperB collaboration, B. O'Leary et al., *SuperB progress reports — physics*, arXiv:1008.1541 [INSPIRE].

[64] T. Aushev et al., *Physics at super B factory*, arXiv:1002.5012 [INSPIRE].

[65] Belle collaboration, K. Ikado et al., *Evidence of the purely leptonic decay* $B^- \to \tau^- \bar{n}u_\tau$, *Phys. Rev. Lett.* **97** (2006) 251802 [hep-ex/0604018] [INSPIRE].

[66] BABAR collaboration, B. Aubert et al., *A search for* $B^+ \to \ell^+\nu_\ell$ *recoiling against* $B^- \to D^0\ell^-\bar{\nu}X$, *Phys. Rev.* **D 81** (2010) 051101 [arXiv:0809.4027] [INSPIRE].

[67] Belle collaboration, K. Hara et al., *Evidence for* $B^- \to \tau^-\bar{\nu}$ *with a semileptonic tagging method*, *Phys. Rev.* **D 82** (2010) 071101 [arXiv:1006.4201] [INSPIRE].

[68] BABAR collaboration, P. del Amo Sanchez et al., *Evidence for* $B^+ - > \tau^+\nu_\tau$ *decays using hadronic B tags*, arXiv:1008.0104 [INSPIRE].

[69] H. Georgi and S. Glashow, *Unity of all elementary particle forces*, *Phys. Rev. Lett.* **32** (1974) 438 [INSPIRE].

[70] R. Slansky, *Group theory for unified model building*, *Phys. Rept.* **79** (1981) 1 [INSPIRE].

[71] H. Georgi and C. Jarlskog, *A new lepton-quark mass relation in a unified theory*, *Phys. Lett.* **B 86** (1979) 297 [INSPIRE].

[72] K. Babu and E. Ma, *Suppression of proton decay in* SU(5) *grand unification*, *Phys. Lett.* **B 144** (1984) 381 [INSPIRE].

[73] A. Giveon, L.J. Hall and U. Sarid, SU(5) *unification revisited*, *Phys. Lett.* **B 271** (1991) 138 [INSPIRE].

[74] I. Doršner and P. Fileviez Perez, *Unification versus proton decay in* SU(5), *Phys. Lett.* **B 642** (2006) 248 [hep-ph/0606062] [INSPIRE].

[75] I. Doršner and I. Mocioiu, *Predictions from type-II see-saw mechanism in* SU(5), *Nucl. Phys.* **B 796** (2008) 123 [arXiv:0708.3332] [INSPIRE].

[76] P. Fileviez Perez, *Renormalizable adjoint* SU(5), *Phys. Lett.* **B 654** (2007) 189 [hep-ph/0702287] [INSPIRE].

[77] I. Doršner, S. Fajfer, J.F. Kamenik and N. Košnik, *Can scalar leptoquarks explain the* f_{D_s} *puzzle?*, *Phys. Lett.* **B 682** (2009) 67 [arXiv:0906.5585] [INSPIRE].

[78] I. Doršner, P. Fileviez Perez and R. Gonzalez Felipe, *Phenomenological and cosmological aspects of a minimal GUT scenario*, *Nucl. Phys.* **B 747** (2006) 312 [hep-ph/0512068] [INSPIRE].

[79] A. Buras, J.R. Ellis, M. Gaillard and D.V. Nanopoulos, *Aspects of the grand unification of strong, weak and electromagnetic interactions*, *Nucl. Phys.* **B 135** (1978) 66 [INSPIRE].

[80] A. De Rujula, H. Georgi and S. Glashow, *Flavor goniometry by proton decay*, *Phys. Rev. Lett.* **45** (1980) 413 [INSPIRE].

JHEP11(2011)002

[81] P. Fileviez Perez, H. Iminniyaz and G. Rodrigo, *Proton stability, dark matter and light color octet scalars in adjoint* SU(5) *unification*, *Phys. Rev.* **D 78** (2008) 015013 [arXiv:0803.4156] [INSPIRE].

[82] B. Bajc, A. Melfo, G. Senjanović and F. Vissani, *Yukawa sector in non-supersymmetric renormalizable* SO(10), *Phys. Rev.* **D 73** (2006) 055001 [hep-ph/0510139] [INSPIRE].

[83] P. Minkowski, $\mu \to e\gamma$ *at a rate of one out of* 1*-billion muon decays?*, *Phys. Lett.* **B 67** (1977) 421 [INSPIRE].

[84] T. Yanagida, *Horizontal symmetry and masses of neutrinos*, in *Proceedings of the Workshop on the Baryon Number of the Universe and Unified Theories*, Tsukuba Japan February 13–14 1979 [INSPIRE].

[85] M. Gell-Mann, P. Ramond and R. Slansky, *Complex spinors and unified theories*, CERN PRINT-80-0576, in *Supergravity Workshop*, Stony Brook U.S.A. September 27–29 1979, pg. 315 [INSPIRE].

[86] S.L. Glashow, *The future of elementary particle physics*, *NATO Adv. Study Inst. Ser. B Phys.* **59** (1980) 687 [INSPIRE].

[87] R.N. Mohapatra and G. Senjanović, *Neutrino mass and spontaneous parity violation*, *Phys. Rev. Lett.* **44** (1980) 912 [INSPIRE].

[88] R. Foot, H. Lew, X. He and G.C. Joshi, *Seesaw neutrino masses induced by a triplet of leptons*, *Z. Phys.* **C 44** (1989) 441 [INSPIRE].

[89] E. Ma, *Pathways to naturally small neutrino masses*, *Phys. Rev. Lett.* **81** (1998) 1171 [hep-ph/9805219] [INSPIRE].

[90] B. Bajc and G. Senjanović, *Seesaw at LHC*, *JHEP* **08** (2007) 014 [hep-ph/0612029] [INSPIRE].

[91] I. Doršner and P. Fileviez Perez, *Upper bound on the mass of the type III seesaw triplet in an* SU(5) *model*, *JHEP* **06** (2007) 029 [hep-ph/0612216] [INSPIRE].

[92] B. Bajc, M. Nemevšek and G. Senjanović, *Probing seesaw at LHC*, *Phys. Rev.* **D 76** (2007) 055011 [hep-ph/0703080] [INSPIRE].

[93] CMS collaboration, V. Khachatryan et al., *Search for pair production of first-generation scalar leptoquarks in pp collisions at* $\sqrt{s} = 7$ *TeV*, *Phys. Rev. Lett.* **106** (2011) 201802 [arXiv:1012.4031] [INSPIRE].

[94] ATLAS collaboration, G. Aad et al., *Search for pair production of first or second generation leptoquarks in proton-proton collisions at* $\sqrt{s} = 7$ *TeV using the ATLAS detector at the LHC*, arXiv:1104.4481 [INSPIRE].

[95] L. Lavoura, H. Kuhbock and W. Grimus, *Charged-fermion masses in* SO(10)*: analysis with scalars in* $10 + 120$, *Nucl. Phys.* **B 754** (2006) 1 [hep-ph/0603259] [INSPIRE].

JHEP11(2011)002